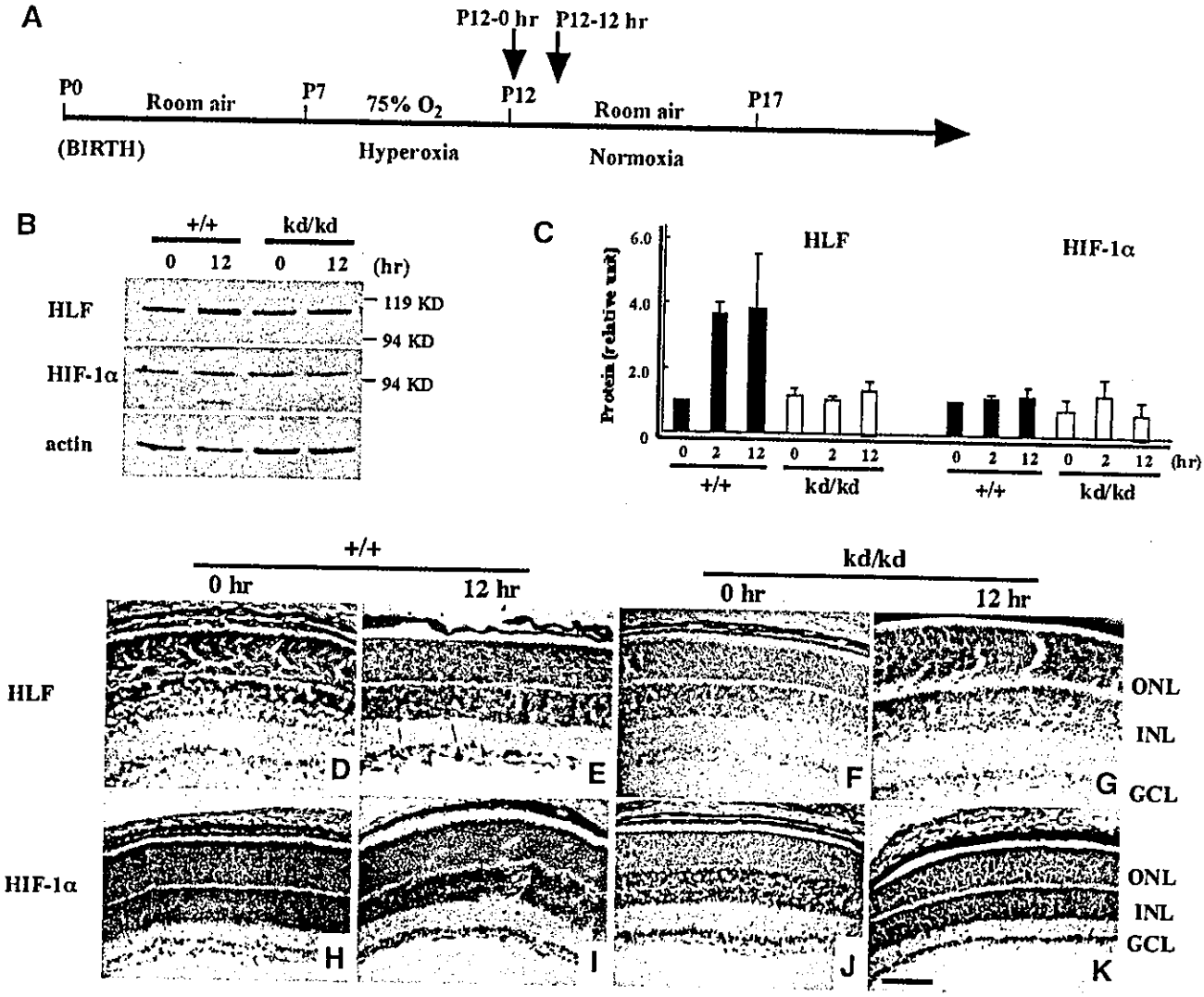

Fig. 3. Expression of protein and immunohistochemical staining of HLF and HIF-1α in retinas. The time course of the experiment is indicated (A). Samples were taken immediately after 75% O_2 treatment (P12–0 h) and 2 and 12 h (P12–12 h) after the shift from 75% O_2 to normal air. Whole-cell extracts were obtained at the appropriate time point (0, 2 and 12 h) and subjected to SDS–PAGE to detect the expression of HLF and HIF-1α (B). Actin antibody was used for detecting the expression of HLF and HIF-1α protein, and HLF and HIF-1α expressions in wild-type mice at P12–0 h were designated as 1.0 (C). Sections of eyeballs from wild-type (+/+) (D, E, H and I) and $HLF^{kd/kd}$ mice (F, G, J and K) at P12–0 h or P12–12 h were incubated with anti-HLF (D–G) and anti-HIF-1α antibody (H–K), and visualized as described in Materials and methods. GCL, ganglion cell layer; ONL, outer nuclear layer; INL, inner nuclear layer.

with an antibody against CD34, a membrane glycoprotein specific for vascular endothelial cells (Young *et al.*, 1995). The formation of neovascular buds was observed on the surface of the GCL of retinas from both wild-type and mutant mice at P12–0 h immediately after shifting from hyperoxic to normoxic conditions, although neovascular buds were clearly fewer in the mutants (Figure 4G and H). After 12 h of normoxic conditions, the neovascular buds were elongated and appeared to infiltrate into the wild-type INL, while in mutant mice they totally disappeared (Figure 4I and J).

Expression of angiogenesis-related genes in the model of ROP

It has been reported that HLF and HIF-1α mRNAs and their proteins are synthesized at almost the same rate under normal O_2 (21%) conditions as they are under hypoxic conditions (Ema *et al.*, 1997). On the other hand, while their proteins were rapidly degraded by the ubiquitin–proteasome system under normoxic conditions, both HLF and HIF-1α proteins were stabilized and accumulated in response to low oxygen concentrations, leading to the enhanced expression of angiogenesis-related genes such as *VEGF*, *VEGFR-1* (*Flt-1*) (Gerber *et al.*, 1997), *VEGFR-2* (*Flk-1*) (Kappel *et al.*, 1999) and *Tie-2* (Tian *et al.*, 1997). We investigated the expression of such genes by RT–PCR and immunohistochemistry. The results from the RT–PCR analysis of various mRNAs were displayed at 25 and 30 reaction cycles, and real-time quantitative PCR was also performed (Figure 5). RT–PCR analysis using total RNA from the mutant mouse eyeballs confirmed the attenuated expression of HLF mRNA as compared with the wild type, even after relative hypoxia treatment. However, no significant elevation of HIF-1α expression was detected in the wild-type or $HLF^{kd/kd}$ mice after relative hypoxia treatment in the real-time quantitative PCR analysis.

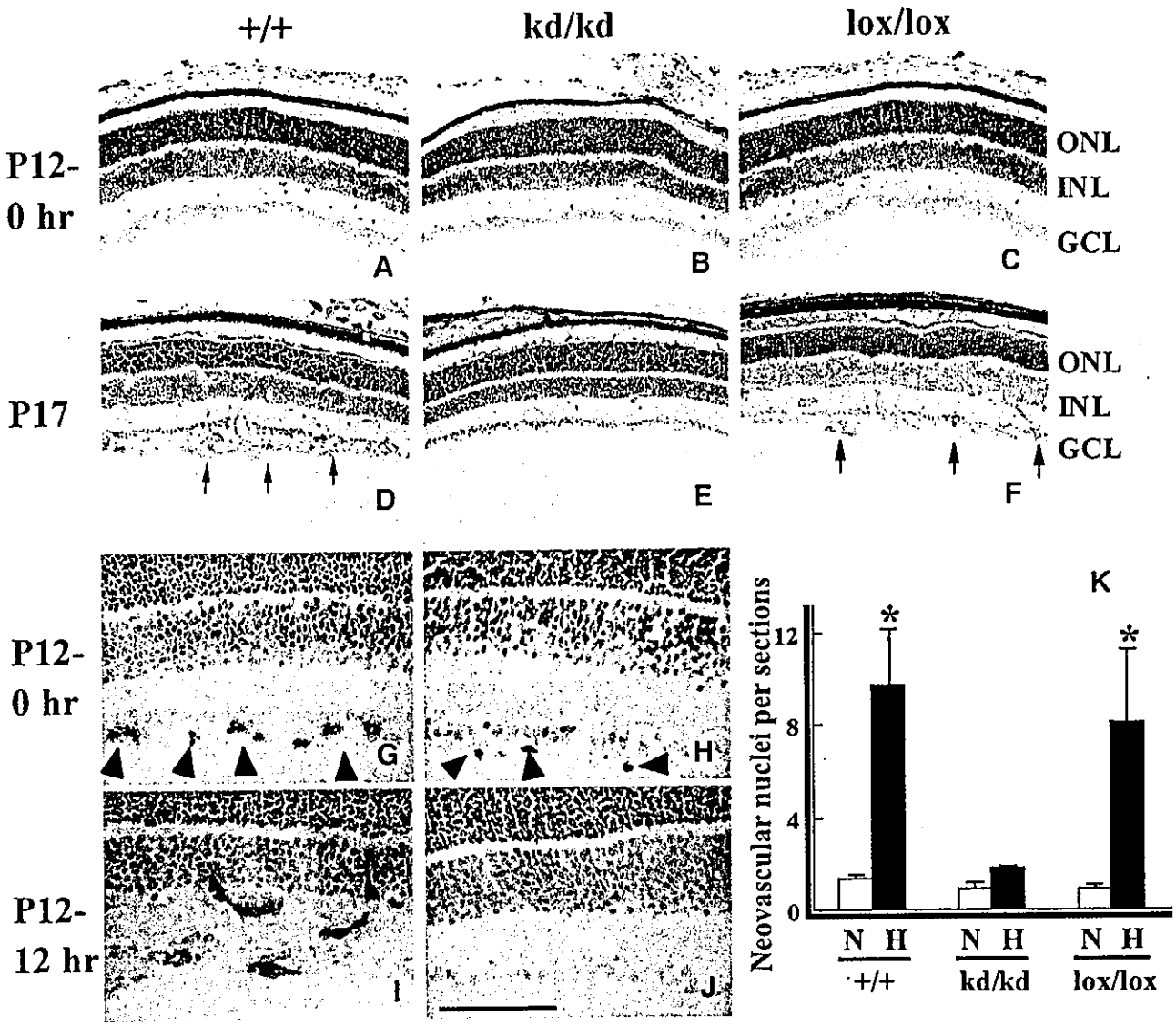

Fig. 4. Neovascularization in the retinas of mice with various genotypes of HLF treated in the model of ROP. Frozen retinal sections from wild-type (+/+), $HLF^{kd/kd}$ (kd/kd) and Cre-recombinase-expressing $HLF^{kd/kd}$ mice (lox/lox) were stained with PAS immediately after the shift from hyperoxia to normoxia (P12–0 h) (A–C). Retinas of $HLF^{+/+}$, $HLF^{kd/kd}$ and $HLF^{lox/lox}$ mice were stained with hematoxylin at P17 (D–F). Arrows indicate numerous clumps of endothelial cells on the surface of the retinas (D and F). Retinas from the $HLF^{+/+}$ and $HLF^{kd/kd}$ mice at P12–0 h and 12 h after shifting from hyperoxia to normoxia (P12–12 h) were subjected to immunostaining with anti-CD34 antibody (G–J). Arrowheads indicate neovascular buds detected in the GCL (G and H). Note that neovascular buds were elongated and infiltrated into the INL (I). Bar indicates 100 μm. Quantification of retinal neovascularization of $HLF^{+/+}$, $HLF^{kd/kd}$ and $HLF^{lox/lox}$ mice at P17 (K). The numbers of neovascular nuclei on the retinal surfaces of $HLF^{+/+}$, $HLF^{kd/kd}$ and $HLF^{lox/lox}$ mice were counted in 250 sections for each of the treated mice and averaged per section. $^*P < 0.01$.

Expression of VEGF mRNA was somewhat upregulated in mice of both genotypes under relative hypoxic conditions as compared with hyperoxic conditions (Figure 5A and E). Immunohistochemistry showed that the protein level of VEGF was significantly elevated by relative hypoxic treatment in both wild-type and $HLF^{kd/kd}$ mice (Figure 6A–C). Thus, it was clearly shown that the mode of VEGF expression was not substantially different between wild-type and $HLF^{kd/kd}$ mice. Immunostainings of VEGF, Epo, Tie-2 and Flk-1 of $HLF^{kd/kd}$ mice at the 0 h point are the same as those of the wild type and deleted from Figure 6.

In sharp contrast, Epo mRNA was enhanced by the relative hypoxia in wild-type mice, while its expression was markedly attenuated even by the successive normoxic treatment in $HLF^{kd/kd}$ mice (Figure 5A and F). This reduced expression of Epo mRNA paralleled that of HLF mRNA in the mutant mice (Figure 5A, C and F). Immunohistochemistry also demonstrated that $HLF^{kd/kd}$ mouse retinas were very weakly stained with anti-Epo antibody compared with the wild-type mice under the relative hypoxic conditions (Figure 6D–F). Other angiogenic factors, such as Flk-1, Flt-1, Tie-1, Tie-2, angiopoietin 1 and angiopoietin 2, were subjected to RT–PCR analysis and essentially no significant difference in their expression levels was observed between $HLF^{kd/kd}$ and wild-type mice (data not shown). In addition, immunostaining showed that the levels of these factors were

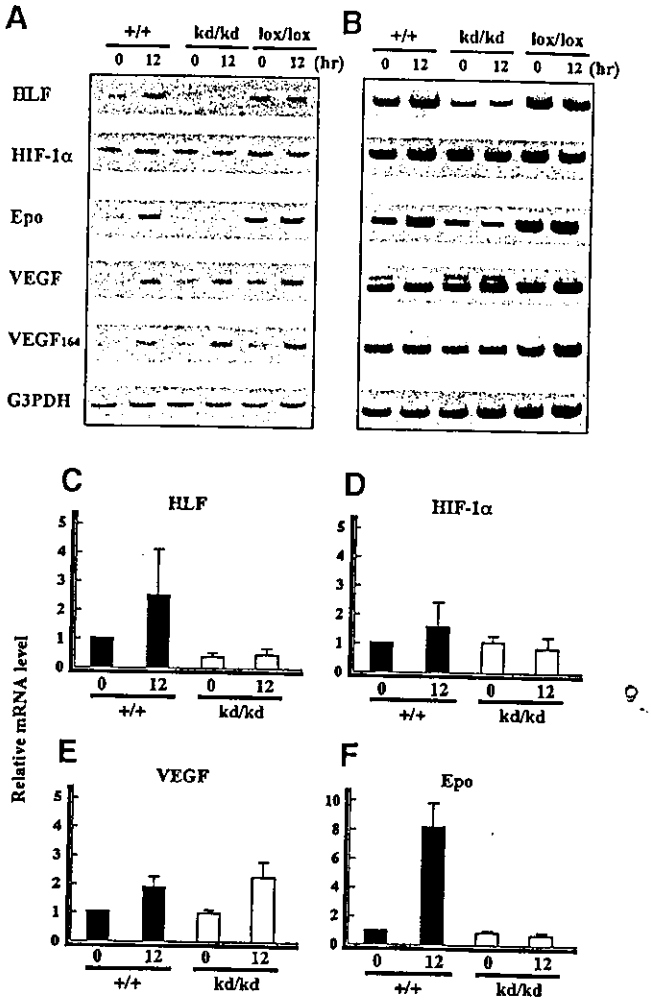

Fig. 5. Expression of angiogenic factors analyzed by RT–PCR. RT–PCR analysis of mRNAs from retinas of $HLF^{+/+}$, $HLF^{kd/kd}$ and $HLF^{lox/lox}$ mice in the model of ROP (P12–0 h, P12–12 h) was undertaken using specific pairs of primers for HLF, HIF-1α, Epo and two forms of VEGF. The results of the PCR analysis are shown at 25 (A) and 30 cycles (B). G3PDH was used as an internal control. Real-time quantitative PCR analysis was also performed for HLF (C), HIF-1α (D), VEGF (E) and Epo (F) in retinas of $HLF^{+/+}$ and $HLF^{kd/kd}$ mice kept in the model of ROP (C–F). The relative mRNA level in $HLF^{+/+}$ mice at P12–0 h is designated as 1.0.

significantly enhanced under relative hypoxic conditions in $HLF^{kd/kd}$ mice as well as in wild-type mice. Immunohistochemistry of VEGF, Flk-1 and Tie-2 displayed different regional expressions, because VEGF is a secretory protein, while Flk-1 and Tie-2 are receptor proteins associated with the plasma membranes of vascular endothelial cells. The expression of VEGF was uniformly enhanced in the GCL and INL of wild-type and mutant retinas exposed to relative hypoxia (Figure 6A–C). In contrast, Tie-2 displayed a rather clustered expression along the extending vascular tubes of wild-type retinas (Figure 6H), while it dispersed rather evenly in $HLF^{kd/kd}$ retinas, probably because no vascular formation developed (Figure 6I). Immunostaining using anti-Flk-1 antibody revealed a similar difference in the distribution of Flk-1 between wild-type and $HLF^{kd/kd}$ mouse retinas to that of Tie-2 (Figure 6K and L). Epo receptor (EpoR) was also expressed in the neovascular tubes of wild-type retinas under relative hypoxic conditions (Figure 6M and O), while EpoR immunostaining was eliminated in the presence of EpoR peptide as a control experiment (Figure 6N).

Association of Epo with neovascularization in the ROP

In order to confirm that Epo is involved in the neovascular process, Epo was injected intraperitoneally into $HLF^{kd/kd}$ mice during relative hypoxia treatment (Figure 7). Neovascular buds appeared in the GCL at P12–12 h in wild-type mice (Figure 7A and B) regardless of Epo administration, whereas neovascular buds were observed in $HLF^{kd/kd}$ mice only when Epo was injected exogenously (Figure 7C and D). Comparison between $HLF^{kd/kd}$ mice treated with or without Epo revealed a significant increase in the number of neovascular buds in the GCL of Epo-treated $HLF^{kd/kd}$ mice [control phosphate-buffered saline (PBS): 1.3 ± 0.2; Epo: 20.4 ± 4.5]. This demonstrated that Epo plays an important role in the formation or maintenance of neovascular buds following a shift from hyperoxic to normoxic conditions. The number of neovascular buds in Epo-injected $HLF^{kd/kd}$ mice did not fully recover to the level of wild type, probably due to the same reasons that administered Epo may not work effectively and/or that some factors other than Epo may also be needed for the formation of neovascular buds.

To further clarify the effect of Epo on neovascularization elongating from the GCL towards the INL, EpoR-deficient mice rescued by intercrossing with transgenic mice expressing *EpoR* transgene under the control of the *GATA-1* promoter (EpoR–/–::Tg+) (Suzuki *et al.*, 2002) were utilized for the ROP model (Figure 7F–H). In these transgenic mice, the expression of EpoR was only detected in hematopoietic organs, such as the spleen and bone marrow, but not in the retina. The number of vascular tubes reaching into the INL of EpoR–/–::Tg+ (Figure 7G and H) at P17 was clearly less than that of the wild type (Figure 7F and H) in which EpoR is expressed normally, suggesting that the Epo/EpoR system is also necessary for neovacularization after relative hypoxic conditions in the retina.

Retinal damage in $HLF^{kd/kd}$ mice during relative hypoxic treatment

At P21 in the ROP model, we found degenerative changes in the inner retinal layer of the $HLF^{kd/kd}$ mice (Figure 8B), which could not be observed at P12 (Figure 4A and B) or P17 (Figure 4D and E), regardless of the *HLF* genotype. Hematoxylin staining of retinal sections from $HLF^{kd/kd}$ mice revealed markedly abnormal retinal structures (Figure 8B), probably resulting from a loss of the INL, as revealed by immunostaining analysis using an anti-vimentin antibody (Figure 8D and E). The expression of vimentin was restricted to the INL, GCL and new vessels of wild-type mice treated with relative hypoxia (Figure 8D). On the other hand, in hypoxia-treated $HLF^{kd/kd}$ mice, immunoreactivity against vimentin was observed only in the GCL and the monolayer (Müller cells) immediately above the GCL, showing that the INL cells almost completely disappeared in these mice (Figure 8B and E). TUNEL analyses revealed continual apoptosis in

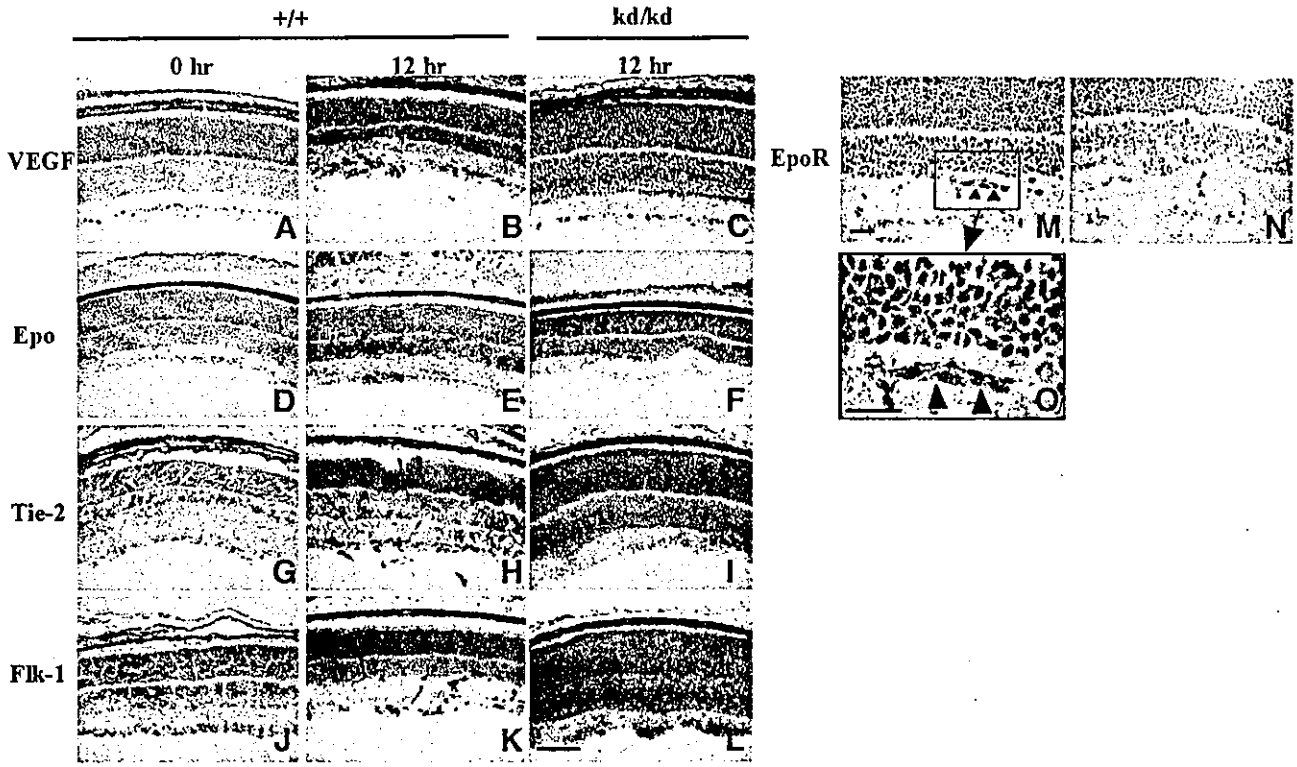

Fig. 6. Immunohistochemical staining with anti-angiogenic factor antibodies. Frozen retinal sections from $HLF^{+/+}$ (A, D, G and J at P12–0 and B, E, H, K, M, N and O at P12–12) and $HLF^{kd/kd}$ mice (C, F, I and L at P12–12) treated in the model of ROP were immunostained with antibodies against VEGF (A–C), Epo (D–F), Tie-2 (G–I), Flk-1 (J–L) and EpoR (M–O). Magnified inserts of the enclosed area (M) are also presented in (O). Arrowheads show endothelial tubes expressing EpoR (M and O). Bars indicate 100 μm (L) and 25 μm (M and O).

the retinal nuclear layers of the $HLF^{kd/kd}$ mice during relative hypoxic treatment. TUNEL analyses of retinas from animals immediately after transfer from hypoxia to normoxia showed frequent induction of apoptosis in both $HLF^{kd/kd}$ and wild-type retinas (data not shown). However, while apoptosis in the wild-type and $HLF^{lox/lox}$ mice was suppressed along with proliferative neovascularization (Figures 8F and H, 4D and F), it was persistently observed in $HLF^{kd/kd}$ mice at P17 (Figure 8G and J). The retinal damage observed in the $HLF^{kd/kd}$ mice was caused at least in part by continued apoptosis due to poor neovascularization.

To examine the physiological function of degenerated retinas in visual synaptic transmission *in vivo*, we analyzed single-flash electroretinogram (ERG) patterns of mouse retinas subjected to the model of ROP. The ERG response to a light flash can be divided into three waves: a-wave, b-wave and OPs (oscillatory potentials consisting of three to four wavelets, OP_1–OP_4), arising from photoreceptors, bipolar cells and amacrine/inner plexiform cells, respectively (Harada *et al.*, 1998). ERG analyses revealed that while the wild-type mice subjected to the model of ROP had a normal flash-light response with a-wave, b-wave and OPs, the $HLF^{kd/kd}$ mice with the degenerative retinas showed a complete loss of b-wave and OPs, but had a normal a-wave amplitude (Figure 8L). These results indicate that $HLF^{kd/kd}$ mice in the model of ROP suffered from functional damage in the neural cells of the INL, but retained functional photoreceptor cells.

Discussion

In order to investigate the functional roles of HLF in adult animals, we produced $HLF^{kd/kd}$ mice by inserting the *neo* gene cassette sandwiched between the two loxP sequences into the first exon encoding the 5′-UTR. The double poly(A) addition signals of the inserted *neo* gene did not work completely, such that leaky transcription reduced the synthesis of HLF mRNA to approximately one-fifth of that in the retinas of wild-type mice.

Under normal conditions, $HLF^{kd/kd}$ newborn mice grow well with apparently normal retinal structures (data not shown), suggesting that this reduced level of HLF production was not harmful to the animals under normal conditions.

The model of ROP is initiated by hyperoxia-induced obliteration of newly formed blood vessels in the retinas of newborn mice (Alon *et al.*, 1995). Subsequently, the retinas of newborn mice become relatively hypoxic when exposed to normal air, because of obliteration of the retinal vessels and induction of abnormal vasoproliferation (Ozaki *et al.*, 1999). In contrast to wild-type mice, proliferative vascularization was not induced in the retinas of $HLF^{kd/kd}$ mice during normoxic conditions preceded by hyperoxic treatment. Although RT–PCR analyses revealed no prominent differences between wild-type and $HLF^{kd/kd}$ mice in their expression of the angiogenic factors VEGF, Flt-1, Flk-1, Tie-1 and Tie-2, only Epo mRNA was notably reduced in $HLF^{kd/kd}$ mice, in parallel with the attenuated

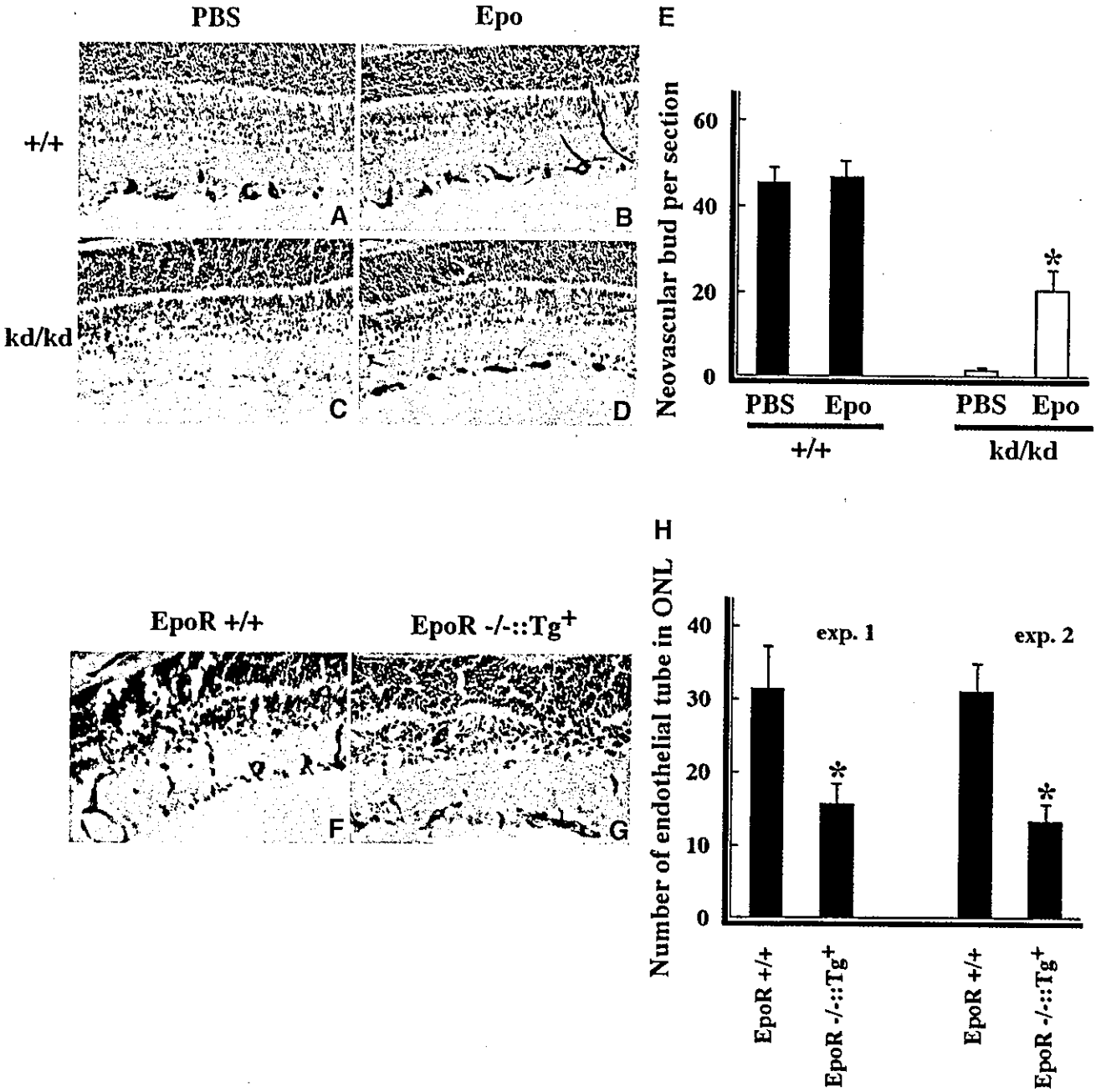

Fig. 7. Effects of Epo on the formation of neovascularization in retinas. $HLF^{+/+}$ and $HLF^{kd/kd}$ mice were kept in the model of ROP and examined for the formation of neovascular buds after administration of control PBS (A and C) and Epo (B and D) at P12–24 h. CD34-positive neovascular buds were scored under the microscope (E). $^*P < 0.01$. After the shift from hyperoxia to normoxia, wild-type (EpoR+/+) mice (F) and EpoR–/–::HG1-EpoR (Tg) mice (G) were examined at P17. The number of neovascular tube formations infiltrated into the INL was counted after the staining with anti-CD34 antibody (H). $^*P < 0.05$.

expression of HLF (Figure 5A, B and F). In $HLF^{lox/lox}$ mice that had the inserted *neo* gene removed by Cre enzyme, the expression of Epo and HLF mRNAs recovered to normal levels, resulting in proliferative neovascularization in response to hypoxic conditions (Figure 4C, F and K). Immunochemical staining of Epo protein displayed similar changes to that of Epo mRNA in wild-type and $HLF^{lox/lox}$ mice, suggesting that Epo is one of the target genes of HLF that is responsible for ROP (Figures 5A, B, F and 6E). This suggestion was strongly supported by the results of the ROP experiments showing that intraperitoneal injection of Epo recovered significant susceptibility in the $HLF^{kd/kd}$ mice to proliferative retinopathy and, conversely, that the EpoR-engineered mice lost the susceptibility to retinopathy to a significant level (Figure 7).

Considering that Epo has been reported to function not only as a hematopoietic, but also as an angiogenic factor (Anagnostou *et al.*, 1990; Ribati *et al.*, 1999), it is very likely that its reduced expression is not sufficient to induce proliferative neovascularization in $HLF^{kd/kd}$ mice. Needless to say, we cannot rigorously rule out the possibility that factors other than Epo, which are

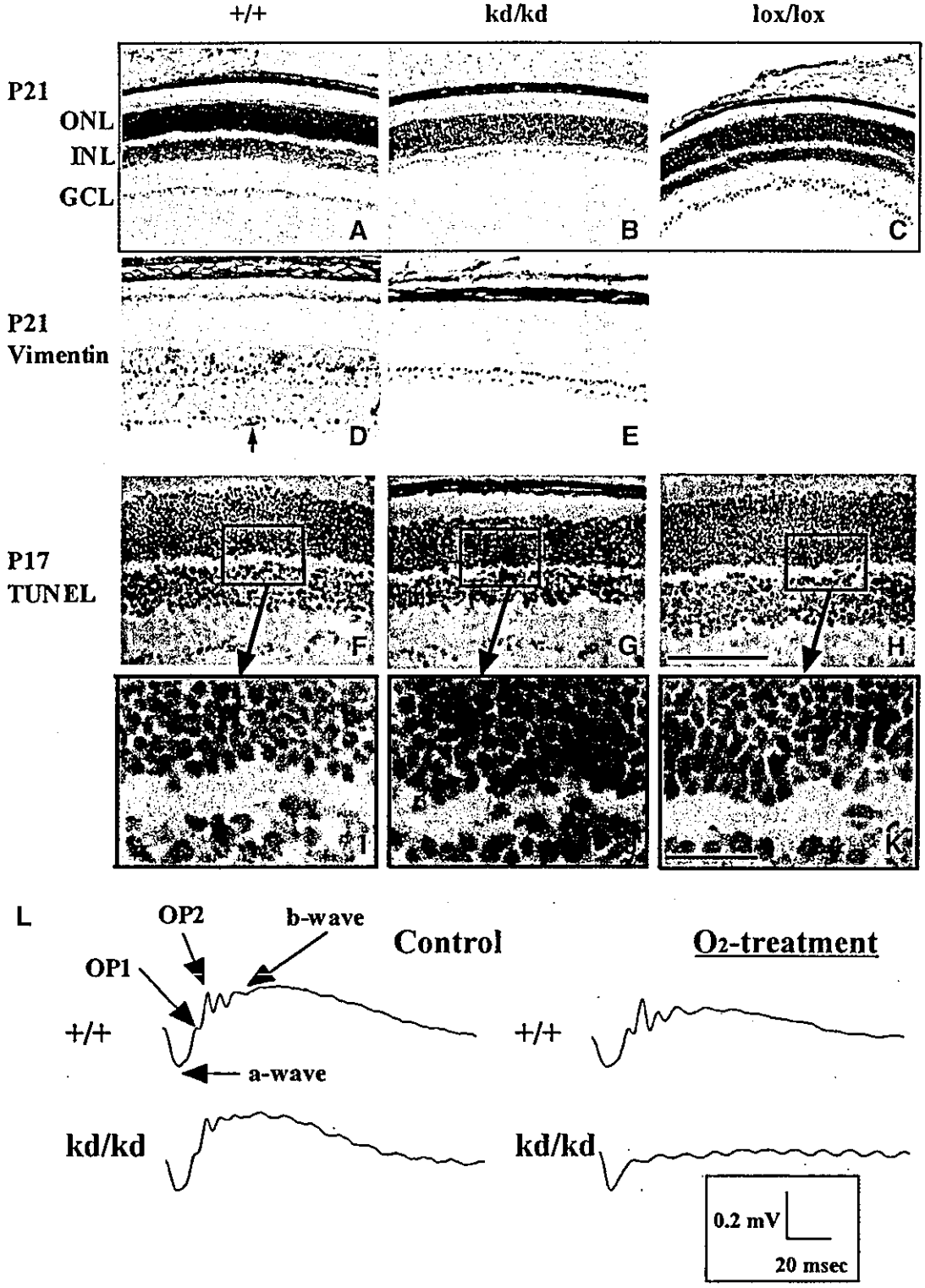

Fig. 8. Structural and functional alterations induced in retinas from $HLF^{kd/kd}$ mice (P21) by prolonged normoxia treatment after hyperoxia. Hematoxylin-stained retinas of $HLF^{+/+}$, $HLF^{kd/kd}$ and $HLF^{lox/lox}$ mice (P21) exposed to prolonged normoxia treatment following hyperoxia (A–C). Immunohistochemical staining of retinas from $HLF^{+/+}$ and $HLF^{kd/kd}$ mice (P21) with an anti-vimentin antibody (D and E). Note that loss of the INL from $HLF^{kd/kd}$ retinas is presented (B). An arrow shows newly formed blood vessel in the retina (D). TUNEL reactions of retinal sections from $HLF^{+/+}$, $HLF^{kd/kd}$ and $HLF^{lox/lox}$ mice at P17 (F–H). Magnified inserts of the enclosed areas are also presented (I–K). Retinal sections were subjected to the TUNEL reaction and followed by counterstaining with Nuclear Fast Red. Bars indicate 100 μm (H) and 25 μm (K). ERGs of $HLF^{+/+}$ and $HLF^{kd/kd}$ mice at P21 in the model of ROP (L). Three animals from each experimental group were used.

Table I. Primers used for the PCR

VEGF	5′ primer	5′-CTTCCTACAGCACAGCAGATGTGAA-3′
	3′ primer	5′-TGGTGAATGGTTAATCGGTCTTTC-3′
VEGF164	5′ primer	5′-CTTTACTGCTGTACCTTCACCATGC-3′
	3′ primer	5′-AACAAGGCTCACAAGTGATTTTCTGG-3
Epo	5′ primer	5′-TGGCACCCTGCTGCTTTTACTCTCCTT-3′
	3′ primer	5′-CTGGAGGCGACATCAATTCCTTCTGAG-3′
EpoR	5′ primer	5′-TCTTCACCACCCACAAGGGTAACTTCCA-3′
	3′ primer	5′-AGATGCCAGAATCGGACACCACAAGGTA-3′
Tie2	5′ primer	5′-CGTCAACAAGCATCCTTCCTACCTGCTA-3′
	3′ primer	5′-TGCATCCTTCTGGTCCACTACACCTTTC-3′
HLF	5′ primer	5′-CAGCTCAGAGCTGAGGAAGG-3′
	3′ primer	5′-GTTGTAGACTCACTTGCC-3′
HIF-1α	5′ primer	5′-CAAGATCTCGGCGAACGAAAGAGTCTGA-3′
	3′ primer	5′-GAAGCACCTTCCACGTTGCTGACTTGAT-3′.
Flt-1	5′ primer	5′-TCTTGCTCACCATGGTCAGC-3′
	3′ primer	5′-GTCATGTGCACAAGTTTGGG-3′
Flk-1	5′ primer	5′-TCGCTCTGTGGTTCTGCGTG-3′
	3′ primer	5′-GGTTTGAAATCGACCCTCGG-3′
G3PDH	5′ primer	5′-TGAAGGTCGGTGTGAACGGATTTGGC-3′
	3′ primer	5′-CATGTAGGCCATGAGGTCCACCAC-3′.

specifically regulated by HLF, are involved in proliferative vascularization. Despite its normal expression in *HLF*$^{kd/kd}$ mice, HIF-1α cannot functionally compensate for HLF in this process, while Epo gene expression is known to be regulated by both HIF-1α and HLF through the HRE located downstream of the gene by DNA transfection assays (Wanner *et al.*, 2000). It remains to be elucidated why only HLF, but not HIF-1α, transactivates the expression of the Epo gene in the retinas of ROP.

During prolonged exposure to normoxia following hyperoxic treatment, the structure of the *HLF*$^{kd/kd}$ retinas displayed not only suppression of neovascularization, but also a prominent degenerative change in the INL at P21, probably resulting from prolonged hypoxia due to poor neovascularization. It was recently reported that Epo plays a protective role in neurons against apoptosis in cerebral ischemia (Digicaylioglu and Lipton, 2001; Siren *et al.*, 2001). Indeed, expression of the EpoR was detected in the INL and neovasculature of wild-type mice (Figure 6M and N), suggesting that reduced Epo synthesis in *HLF*$^{kd/kd}$ retinas exposed to relative hypoxia may aggravate degeneration of the INL due to defective neural protection and poor neovascular formation. Localized expression of Epo in the retina is thought to be important in protecting nuclear layers, because Epo concentrations in the blood sera did not differ between *HLF*$^{kd/kd}$ and wild-type mice under normoxic conditions (data not shown).

Single-flash ERG analyses revealed that *HLF*$^{kd/kd}$ mice lost b-wave and OPs mainly derived from bipolar cells and the amacrine/interplexiform during the prolonged relative hypoxic treatment (Figure 8L). In contrast, wild-type mice undergoing the same treatment retained normal neurotransmission of light response, indicating that at least the Epo gene under the control of HLF may play a critical role in protection against degeneration of the INL in the ROP model.

VEGF is thought to represent a major factor triggering neovascularization in the retina of relative hypoxia (Aiello *et al.*, 1995; Seo *et al.*, 1999). Indeed, VEGF was expressed in the INL and GCL in response to hypoxia, and its receptor Flk-1 was also expressed in the elongated endothelial cells (Figure 6K), confirming that the VEGF/Flk-1 interaction induces proliferation of the retinal vasculature. Although neovascular bud formation was transiently observed immediately after hypoxia treatment, *HLF*$^{kd/kd}$ mice did not develop any vascular formation from these buds during treatment with hypoxia, even with a production of VEGF equivalent to that in wild-type mice (Figures 5E and 6). The results indicated that some factors other than VEGF are also necessary for induction of neovascularization and that Epo may be one of the factors that plays a protective or anti-apoptotic role in endothelial cell buds (Carlini *et al.*, 1999) during neovasculogenesis in the ROP. Therefore, it would be interesting to investigate how Epo and VEGF interplay in the development of neovascularization in response to hypoxia. Recently, inhibitory PAS (IPAS) protein, which acts as a dominant-negative regulator of HIFs, was isolated by Makino *et al.* (2001). IPAS is expressed in response to hypoxia and inhibits the activities of HLF and HIF-1α in both corneal epithelium and retinal GCL and INL, suggesting a more complicated regulatory mechanism for neovascularization observed in the ROP.

Consequently, in addition to VEGF, Epo was found to be a key factor in the ROP, especially in the development of neovascularization, suggesting a therapeutic possibility of Epo and VEGF inhibitors in the ROP. *HLF*$^{kd/kd}$ mice have turned out to be very useful for investigation of the physiological roles of HLF and might also shed light on the function of HLF that is distinct from that of HIF-1α in terms of vascularization and angiogenesis under hypoxic conditions.

Materials and methods

HLF gene targeting

A genomic DNA sequence extending from the first exon to 5.1 and 2.7 kb in the 5′ and 3′ directions, respectively, was cloned from a 129/SV mouse genomic library and used for construction of a targeting vector. A

neomycin resistance gene (*neo*) cassette sandwiched between loxP sequences was inserted into the first exon of the *HLF* gene. The constructed chimeric DNA was then cloned into pUC18. The targeting vector was amplified, linearized by *Not*I digestion and electroporated into E14 cells. The electroporated cells were subjected to double selection in G418 (300 μg/ml) and gancyclovir (1 μg/ml), and amplified. After 10 days, colonies were isolated, expanded and screened for homologous recombination by the PCR method. DNA from an isolated double-resistant clone was further confirmed for homologous recombination by DNA blot analysis. Double-resistant ES cells were injected into C57BL/6J blastocysts that were surgically implanted into the uterus of pseudopregnant ICR foster mothers. Chimeric mice were then intercrossed with C57BL/6J mice and the offspring were genotyped.

Murine model of retinal neovascularization

The murine hyperoxia–normoxia-induced proliferative retinopathy model established by Smith (1994) was used in this study. Briefly, at P7, 20 littermates from each group of $HLF^{kd/kd}$ and wild-type mice, along with nursing mothers, were exposed to 75% oxygen for 5 days, and at P12 the animals were returned to room air (21% O_2). Following exposure to room air, a certain number of mice (the number is indicated in parentheses for each time point) were killed at one of the following time points: 0 h (3), 2 h (3), 12 h (3), 24 h (3), 36 h (2), 5 days (P17) (3) and 9 days (P21) (3). An oxygen-enriched atmosphere was obtained by mixing air with oxygen, and oxygen levels were monitored using a polarographic oxygen sensor (Teijin, Tokyo, Japan). Eyeballs were rapidly removed and embedded in an optimal cutting medium (O.C.T. Compound; Sakura, Tokyo, Japan) for histochemical and immunostaining analyses. The treated mice were kept with nursing mothers under normal conditions and eyes were removed at P17 under Nembutal anesthesia for histochemical and immunochemical analyses. Frozen retinal sections were cut at 5 μm for immunohistochemistry and periodic and acid Schiff stain (PAS) and hematoxylin staining.

Immunohistochemistry and electroretinogram analysis

Frozen sections of eyes were immunohistochemically stained using anti-HIF-1α, Epo, Tie-2, VEGF, Flk-1 EpoR (Santa Cruz Biotechnology, Santa Cruz, CA), vimentin (Nichirei, Tokyo, Japan) and CD34 (Young *et al.*, 1995) antibodies. To obtain anti-HLF antibody, two rabbits were immunized with the synthetic 16 amino acids of the C-terminus of mouse HLF (656–671 amino acids), and the resulting bleed was affinity purified (Sawady Technology Inc., Tokyo, Japan). The specificity of the anti-HLF antibody was examined by ELISA and western blot analyses.

The sections were fixed in 4% paraformaldehyde/PBS for 15 min, washed twice with PBS and incubated for 30 min with 10% normal goat serum. The slides were then incubated overnight at 4°C with respective specific antibodies or non-immune serum. After washing with PBS, the slides were further incubated with biotinylated goat anti-rabbit IgG antibody (Vector Laboratories, Inc., Burlingame, CA), followed by streptavidin-conjugated ABC complex (Vector Laboratories) or horseradish peroxidase (HRP)-conjugated goat anti-rabbit IgG antibody (Biosource, Camarillo, CA). Specific staining was visualized by incubation with 3,3′-diaminobenzidine. Counterstaining was carried out using Nuclear Fast Red.

Electroretinogram analysis was performed as described previously (Abe *et al.*, 1999).

RT–PCR

Total RNA was prepared from eyeballs of mice with various genotypes of the HLF gene using RNA isolation reagent (Trizol, Invitrogen). cDNAs were synthesized using a RT–PCR kit (Clontech Laboratories) in a reaction solution (20 μl) containing total RNA (1 μg) prepared from eyeballs of mice treated in various ways. An aliquot (1 μl) of synthesized cDNA was amplified (Clontech Laboratories) in a total volume of 20 μl containing 150 mM dNTP, 0.2 U of *Taq* polymerase and 0.12 μg of each pair of primers. The PCR procedure consisted of 25 or 30 cycles of the reaction: 95°C for 30 s and 68°C for 1 min. The PCR products were electrophoretically separated on 2% agarose gels. In addition, cDNA was amplified and quantified using an ABI Prism 7700 Sequence Detector (Parkin Elmer, Foster City, CA). The primers used for the PCR reaction are listed in Table I.

Western blot analysis

Mouse eyeballs were lysed with lysis buffer [10 mM HEPES pH 7.9, 10 mM potassium chloride, 0.1 mM EDTA, 1 mM dithiothreitol, 1% NP-40 and protease inhibitor cocktail (Roche, Mannheim, Germany)]. Whole-cell extracts (100 μg) were resolved in 10% SDS–polyacrylamide gels and electrophoretically transferred onto a polyvinylidene difluoride membrane (Millipore, Bedford, MA). For HLF detection, rabbit anti-HLF antibody was used and, for HIF-1α, anti-HIF-1α antibody (H1α67; Lab Vision, Fremont, CA) was used. Detection was performed with HRP-conjugated goat anti-rabbit or rabbit anti-goat immunoglobulins (Biosource) and enhanced chemiluminescence (ECL; Amersham Biosciences, UK). After analysis, goat anti-actin antibody (I-19; Santa Cruz Biotechnology, Santa Cruz, CA) was used to verify equal protein loading and transfer.

TUNEL assay

The TUNEL assay was performed using an *in situ* apoptosis detection kit (TaKaRa, Code No. MK500) as specified by the manufacturer. Frozen eye sections (5 μm) were fixed in 4% paraformaldehyde/PBS for 30 min and washed with PBS for 10 min at room temperature (RT). Slides were treated with 0.3% hydrogen peroxide in methanol for 30 min at RT and incubated with permeabilization buffer for 5 min on ice. Subsequently, the samples were incubated with reaction buffer overnight at 4°C. After several washings with PBS, sections were incubated with anti-FITC–HRP conjugate for 30 min at 37°C and washed with PBS. Staining was performed using diaminobenzidine and samples were counterstained with Nuclear Fast Red.

Epo injection

To investigate the role of Epo in neovascularization, Epo (a generous gift from Chugai Pharmaceutical Co., Tokyo, Japan) was intraperitoneally injected into neonates (5000 IU/kg) (Grimm *et al.*, 2002) at P12–0 h and P12–12 h. The effect of Epo on the formation of neovascular buds was evaluated by scoring the number of buds observed in the GCL at P12–24 h after staining with anti-CD34 antibody.

EpoR–/–::HG1-EPOR (Tg) mice were obtained by crossing EpoR+/–::Tg mice with EpoR+/– mice, as reported previously (Suzuki *et al.*, 2002), and newborn mice were exposed to 75% oxygen for 5 days and subsequently returned to room air. Mice were analyzed at P17 for neovascularization by staining with anti-CD34 antibody, and the number of tube formations reaching the INL were scored under the microscope.

Acknowledgements

The authors would like to thank Drs K.Gradin (Tohoku University) and T.O'Connor (University of Tsukuba) for critical reading of the manuscript, Drs K.Araki and K.Yamamura (Kumamoto University) for the Cre-expressing transgenic mice, K.Yasumoto (Tohoku University) for kind help and suggestions and Ms N.Kaneko (University of Tsukuba) for histological analyses. Our hearty thanks are also due to Ms S.Suzuki, M.Irie and Mr H.Abe for secretarial and graphic work. This work was supported in part by a Grant-in-Aid for Scientific Research of Priority Area (A) of the Ministry of Education, Science, Sports and Culture of Japan, funds for Research for the Future Program of the Japan Society for the Promotion of Science and for Core Research for Evolution Science of Japan Science and Technology Corporation, for Program for Promotion of Basic Research Activities for Innovative Biosciences, for Project of Exploratory Research for Advanced Technology of JST and a fund from Sankyo Co.

References

Abe,T. *et al.* (1999) Functional analysis after auto iris pigment epithelial cell transplantation in patients with age-related macular degeneration. *Tohoku J. Exp. Med.*, **189**, 295–305.

Aiello,L.P., Pierce,E.A., Foley,E.D., Takagi,H., Chen,H., Riddle,L., Ferrara,N., King,G.L. and Smith,L.E. (1995) Suppression of retinal neovascularization *in vivo* by inhibition of vascular endothelial growth factor (VEGF) using soluble VEGF–receptor chimeric proteins. *Proc. Natl Acad. Sci. USA*, **92**, 10457–10461.

Alon,T., Hemo,I., Itin,A., Pe'er,J., Stone,J. and Keshet,E. (1995) Vascular endothelial growth factor acts as a survival factor for newly formed retinal vessels and has implications for retinopathy of prematurity. *Nat. Med.*, **10**, 1024–1028.

Anagnostou,A., Lee,E.S., Kessimian,N., Levinson,R. and Steiner,M. (1990) Erythropoietin has a mitogenic and positive chemotactic effect on endothelial cells. *Proc. Natl Acad. Sci. USA*, **87**, 5978–5982.

Carlini,R.G., Alonzo,E.J., Dominguez,J., Blanca,I., Weisinger,J.R., Rothstein,M. and Bellorin-Font,E. (1999) Effect of recombinant

human erythropoietin on endothelial cell apoptosis. *Kidney Int.*, 55, 546–553.

Digicaylioglu,M. and Lipton,S.A. (2001) Erythropoietin-mediated neuroprotection involves cross-talk between Jak2 and NF-κB signaling cascades. *Nature*, 412, 641–647.

Ema,M., Taya,S., Yokotani,N., Sogawa,K., Matsuda,Y. and Fujii-Kuriyama,Y. (1997) A novel bHLH–PAS factor with close sequence similarity to hypoxia-inducible factor 1α regulates the VEGF expression and is potentially involved in lung and vascular development. *Proc. Natl Acad. Sci. USA*, 94, 4273–4278.

Epstein,A.C. *et al.* (2001) *C.elegans* EGL-9 and mammalian homologs define a family of dioxygenases that regulate HIF by prolyl hydroxylation. *Cell*, 107, 43–54.

Firth,J.D., Ebert,B.L., Pugh,C.W. and Ratcliffe,P.J. (1994) Oxygen-regulated control elements in the phosphoglycerate kinase 1 and lactate dehydrogenase A genes: similarities with the erythropoietin 3′ enhancer. *Proc. Natl Acad. Sci. USA*, 91, 6496–6500.

Forsythe,J.A., Jiang,B.H., Iyer,N.V., Agani,F., Leung,S.W., Koos,R.D. and Semenza,G.L. (1996) Activation of vascular endothelial growth factor gene transcription by hypoxia-inducible factor 1. *Mol. Cell. Biol.*, 16, 4604–4613.

Gerber,H.P., Condorelli,F., Park,J. and Ferrara,N. (1997) Differential transcriptional regulation of the two vascular endothelial growth factor receptor genes. Flt-1, but not Flk-1/KDR, is up-regulated by hypoxia. *J. Biol. Chem.*, 272, 23659–23667.

Grimm,C., Wenzel,A., Groszer,M., Mayser,H., Seeliger,M., Samardzija,M., Bauer,C., Gassmann,M. and Reme,C.E. (2002) HIF-1-induced erythropoietin in the hypoxic retina protects against light-induced retinal degeneration. *Nat. Med.*, 8, 718–724.

Harada,T. *et al.* (1998) Functions of the two glutamate transporters GLAST and GLT-1 in the retina. *Proc. Natl Acad. Sci. USA*, 95, 4663–4666.

Iyer,N.V. *et al.* (1998) Cellular and developmental control of O_2 homeostasis by hypoxia-inducible factor 1α. *Genes Dev.*, 12, 149–162.

Jain,S., Maltepe,E., Lu,M.M., Simon,C. and Bradfield,C.A. (1998) Expression of ARNT, ARNT2, HIF-1α, HIF-2α and Ah receptor mRNAs in the developing mouse. *Mech. Dev.*, 73, 117–123.

Kallio,P.J., Wilson,W.J., O'Brien,S., Makino,Y. and Poellinger,L. (1999) Regulation of the hypoxia-inducible transcription factor 1α by the ubiquitin–proteasome pathway. *J. Biol. Chem.*, 274, 6519–6525.

Kappel,A., Ronicke,V., Damert,A., Flamme,I., Risau,W. and Breier,G. (1999) Identification of vascular endothelial growth factor (VEGF) receptor-2 (Flk-1) promoter/enhancer sequences sufficient for angioblast and endothelial cell-specific transcription in transgenic mice. *Blood*, 93, 4284–4289.

Liu,Y., Cox,S.R., Morita,T. and Kourembanas,S. (1995) Hypoxia regulates vascular endothelial growth factor gene expression in endothelial cells. Identification of a 5′ enhancer. *Circ. Res.*, 77, 638–643.

Makino,Y., Cao,R., Svensson,K., Bertilsson,G., Asman,M., Tanaka,H., Cao,Y., Berkenstam,A. and Poellinger,L. (2001) Inhibitory PAS domain protein is a negative regulator of hypoxia-inducible gene expression. *Nature*, 414, 550–554.

Moss,S.E., Klein,R. and Klein,B.E. (1994) Ten-year incidence of visual loss in a diabetic population. *Ophthalmology*, 101, 1061–1070.

Niwa,H., Araki,K., Kimura,S., Taniguchi,S., Wakasugi,S. and Yamamura,K. (1993) An efficient gene-trap method using poly A trap vectors and characterization of gene-trap events. *J. Biochem.*, 113, 343–349.

Okamoto,N., Okamoto,N., Tobe,T., Hackett,S.F., Ozaki,H., Vinores,M.A., LaRochelle,W., Zack,D.J. and Campochiaro,P.A. (1997) Transgenic mice with increased expression of vascular endothelial growth factor in the retina: a new model of intraretinal and subretinal neovascularization. *Am. J. Pathol.*, 151, 281–291.

Ozaki,H. *et al.* (1999) Hypoxia inducible factor-1α is increased in ischemic retina: temporal and spatial correlation with VEGF expression. *Invest. Ophthalmol. Vis. Sci.*, 40, 182–189.

Peng,J., Zhang,L., Drysdale,L. and Fong,G.H. (2000) The transcription factor EPAS-1/hypoxia-inducible factor 2α plays an important role in vascular remodeling. *Proc. Natl Acad. Sci. USA*, 97, 8386–8391.

Pierce,E.A., Avery,R.L., Foley,E.D., Aiello,L.P. and Smith,L.E. (1995) Vascular endothelial growth factor/vascular permeability factor expression in a mouse model of retinal neovascularization. *Proc. Natl Acad. Sci. USA*, 92, 905–909.

Prost,M. (1988) Experimental studies on the pathogenesis of retinopathy of prematurity. *Br. J. Ophthalmol.*, 72, 363–367.

Ribati,D., Presta,M., Vacca,A., Ria,R., Giuliani,R., Dell'Era,P., Nico,B., Roncali,L. and Dammacco,F. (1999) Human erythropoietin induces a pro-angiogenic phenotype in cultured endotherial cells and stimulates neovascularization *in vivo*. *Blood*, 93, 2627–2636.

Ryan,H.E., Lo,J. and Johnson,R.S. (1998) HIF-1α is required for solid tumor formation and embryonic vascularization. *EMBO J.*, 17, 3005–3015.

Semenza,G.L. and Wang,G.L. (1992) A nuclear factor induced by hypoxia via *de novo* protein synthesis binds to the human erythropoietin gene enhancer at a site required for transcriptional activation. *Mol. Cell. Biol.*, 12, 5447–5454.

Seo,M.S. *et al.* (1999) Dramatic inhibition of retinal and choroidal neovascularization by oral administration of a kinase inhibitor. *Am. J. Pathol.*, 154, 1743–1753.

Siren,A.-L. *et al.* (2001) Erythropoietin prevents neural apoptosis after cerebral ischemia and metabolic stress. *Proc. Natl Acad. Sci. USA*, 98, 4044–4049.

Smith,L.E., Wesolowski,E., McLellan,A., Kostyk,S.K., D'Amato,R., Sullivan,R. and D'Amore,P.A. (1994) Oxygen-induced retinopathy in the mouse. *Invest. Ophthalmol. Vis. Sci.*, 35, 101–111.

Suzuki,N., Ohneda,O., Takahashi,S., Higuchi,M., Mukai,H.Y., Nakahata,T., Imagawa,S. and Yamamoto,M. (2002) Erythroid-specific expression of the erythropoietin receptor rescued its null mutant mice from lethality. *Blood*, 100, 2279–2288.

Tian,H., McKnight,S.L. and Russell,D.W. (1997) Endothelial PAS domain protein 1 (EPAS1), a transcription factor selectively expressed in endothelial cells. *Genes Dev.*, 11, 72–82.

Tian,H., Hammer,R.E., Matsumoto,A.M., Russell,D.W. and McKnight,S.L. (1998) The hypoxia-responsive transcription factor EPAS1 is essential for catecholamine homeostasis and protection against heart failure during embryonic development. *Genes Dev.*, 12, 3320–3324.

Tobe,T., Okamoto,N., Vinores,M.A., Derevjanik,N.L., Vinores,S.A., Zack,D.J. and Campochiaro,P.A. (1998) Evolution of neovascularization in mice with overexpression of vascular endothelial growth factor in photoreceptors. *Invest. Ophthalmol. Vis. Sci.*, 39, 180–188.

Wang,G.L. and Semenza,G.L. (1993) General involvement of hypoxia-inducible factor 1 in transcriptional response to hypoxia. *Proc. Natl Acad. Sci. USA*, 90, 4304–4308.

Wang,G.L., Jiang,B.H., Rue,E.A. and Semenza,G.L. (1995) Hypoxia-inducible factor 1 is a basic-helix–loop–helix PAS heterodimer regulated by cellular O_2 tension. *Proc. Natl Acad. Sci. USA*, 92, 5510–5514.

Wanner,R.M. *et al.* (2000) Epolones induce erythropoietin expression via hypoxia-inducible factor-1α activation. *Blood*, 96, 1558–1565.

Wenger,R.H. and Gassmann,M. (1997) Oxygen(es) and the hypoxia-inducible factor-1. *Biol. Chem.*, 378, 609–616.

Young,P.E., Baumhueter,S. and Lasky,L.A. (1995) The sialomucin CD34 is expressed on hematopoietic cells and blood vessels during murine development. *Blood*, 85, 96–105.

Received March 12, 2002; revised October 24, 2002; accepted January 14, 2003

ELSEVIER

Biochimica et Biophysica Acta 1619 (2003) 263–268

BIOCHIMICA ET BIOPHYSICA ACTA
BBA
www.bba-direct.com

Review

Functional role of AhR in the expression of toxic effects by TCDD

Junsei Mimura[a,1], Yoshiaki Fujii-Kuriyama[a,b,*,1]

[a] *Department of Biomolecular Science, Graduate School of Life Science, Tohoku University, Aoba-ku, Sendai 980-8578, Japan*
[b] *Core Research for Evolutional Science and Technology (CREST), Japan Science and Technology Corporation, Japan*

Received 25 March 2002; accepted 6 June 2002

Abstract

Cytochrome P450 1A1 (*CYP1A1*) is one of the xenobiotic metabolizing enzymes (XMEs), which is induced by polycyclic aromatic hydrocarbons (PAHs). The most potent inducer of *CYP1A1* is 2,3,7,8-tetrachlorodibenzo-*p*-dioxin (TCDD). In addition, TCDD induces a broad spectrum of biochemical and toxic effects, such as teratogenesis, immunosuppression and tumor promotion. Most, if not all, of the effects caused by TCDD and other PAHs are known to be mediated by AhR (aryl hydrocarbon receptor or dioxin receptor) which has a high binding affinity to TCDD. The liganded AhR translocates from cytoplasm to nuclei where it switches its partner molecule from Hsp90 to Arnt. Thus formed AhR/Arnt heterodimer binds a specific DNA sequence designated XRE in the promoter region of the target genes including *CYP1A1*, *UDP-glucuronosyl transferase* and others to enhance their expression. Although it remains to be studied how AhR is involved in the other TCDD-induced biological effects such as teratogenesis and immunosuppression than induction of XMEs, it is believed that these adverse TCDD effects are caused by untimely activation of gene expression by ligand-activated AhR in the biological process. We summarize the present knowledge about functional role of AhR in TCDD-induced biological effects.

Keywords: Arylhydrocarbon receptor; 2,3,7,8-Tetrachlorodibenzo-*p*-dioxin; *CYP1A1*

1. Introduction

Cytochrome P450 1A1 (*CYP1A1*) is a member of a multigene family of xenobiotic metabolizing enzymes (XMEs) [1]. Beside its physiological role in the detoxification of polycyclic aromatic compounds, the activity of this enzyme can be deleterious since it generates mutagenic metabolites and active oxygen [2]. These polycyclic aromatic hydrocarbons (PAHs) enhance *CYP1A1* activity by activating the transcription of the *CYP1A1* gene. Although many CYP genes which are involved in metabolism of foreign chemicals are transcriptionally activated by their specific member of nuclear receptor superfamily (CAR, PXR, PPAR and so on), the induction of *CYP1A1* gene is regulated by aryl hydrocarbon receptor (AhR), a bHLH-PAS transcription factor that is structurally distinct from the nuclear receptor superfamily [3–6]. In the absence of ligand, AhR is present in the cytosol in a complex with Hsp90, XAP2 and p23 proteins. Upon binding to a ligand, the AhR complex translocates into the nucleus and the AhR dissociates from Hsp90 complex to form a heterodimer with its partner molecule, Arnt. Thus, the formed AhR/Arnt heterodimer recognizes an enhancer DNA element designated xenobiotic responsive element (XRE) sequence located in the promoter region of *CYP1A1* gene, resulting in the enhanced expression of the gene. In addition to induction of the *CYP1A1* gene, 2,3,7,8-tetrachlorodibenzo-*p*-dioxin (TCDD) causes a broad spectrum of biochemical and toxicological effects, such as teratogenesis, immunosuppression due to thymic involution, and tumor promotion [7]. Extensive studies on the AhR function using AhR-deficient mice have revealed that AhR is responsible for most, if not all, of toxic effects caused by TCDD, besides induction of *CYP1A1* gene and other dioxin-inducible genes [8–10]. This short

Abbreviations: AhR, arylhydrocarbon receptor; CYP, cytochrome P450; XME, xenobiotic metabolizing enzyme; TCDD, 2,3,7,8-tetrachlorodibenzo-*p*-dioxin; PAHs, polycyclic aromatic hydrocarbons; Arnt, AhR nuclear translocator; PAS, Per–Arnt–Sim homology; HSP90, heat shock protein 90 kD; XRE, xenobiotic responsive element; XAP2, hepatitis B virus X-associated protein; RIP140, receptor-interacting protein 140kD; GTFs, general transcription factors; AhRR, AhR repressor; 3-MC, 3-methylchoranthrene; LD_{50}, 50% lethal dose

[1] Present address: Center for Tsukuba Advanced Research Alliance, University of Tsukuba, Tsukuba 305-8577, Japan.

* Corresponding author. Tel.: +81-80-22-217-6590; fax: +81-80-22-217-6594.

E-mail address: ykfujii@mail.cc.tohoku.ac.jp (Y. Fujii-Kuriyama).

0304-4165/02/$ - see front matter
PII: S0304-4165(02)00485-3

review summarizes briefly the present knowledge of AhR functions in the biological effects of TCDD. Because of a limited space, we apologize that we could not comprehensively refer to all the papers that should be referred to.

2. Induction mechanism of *CYP1A1* gene by aromatic hydrocarbon

Among a number of enhancer or silencer elements which affect the expression of *CYP1A1* gene that has been determined, TCDD-induced expression of *CYP1A1* gene is mediated through the XRE (also named DRE or AhRE) sequence [11]. The core consensus sequence of XRE is determined to be 5′-TNGCGTG-3′, and recognized by AhR/Arnt heterodimer. A series of experiments has revealed the mechanisms of AhR-dependent *CYP1A1* gene induction as illustrated in Fig. 1. In the absence of a ligand, AhR exists in a cytosolic complex with Hsp90, co-chaperone p23 and immunophilin-like protein XAP2 (also AIP or ARA9) [12–14]. p23 and XAP2 are thought to be required for maintaining the stability of the hsp90 complex [13,14]. Ligand binding to AhR triggers nuclear translocation of AhR and in the nuclei, liganded AhR replaces its partner molecule with Arnt, resulting in binding to the multiple XREs in the 5′ upstream region of the *CYP1A1* gene. In the case of mouse *CYP1A1* gene, at least six copies of the XRE sequence were identified. Binding of the AhR/Arnt heterodimer to the XREs remodels the chromatin structure and facilitates the association of another transcription factor of Sp1 to its cognate recognition sequence in the promoter region [15,16]. In addition, AhR/Arnt heterodimer directly interacts with Sp1 and the two transcription factors enhance the expression of *CYP1A1* gene synergistically [16]. Transactivation activities of AhR/Arnt heterodimer are transmitted to general transcription factors (GTFs) through interaction with CBP/p300 for Arnt and with RIP140, SRC-1 for AhR as coactivator [17–19]. Phosphorylation state of the AhR/Arnt heterodimer is reported to be also important for transactivation, because the binding activity of the AhR/Arnt heterodimer to the XRE is abolished by the phosphatase treatment [20]. Although the phosphorylation sites of AhR and Arnt were determined to be Tyr^{372} and Ser^{348}, respectively, replacements of these amino acids with Ala had no effect on the DNA binding activity of the heterodimer, indicating that other phosphorylation sites may be responsible for the DNA binding activity [21]. Recently, we have cloned AhR-related factor and termed it AhR repressor (AhRR) [22]. Although AhR needs ligands for nuclear translocation and heterodimerization with Arnt, AhRR localizes in the nuclei and forms a heterodimer with Arnt constitutively. The AhRR/Arnt heterodimer also recognizes the XRE, but functions as a transcriptional repressor. Therefore, AhRR function as a negative regulator of AhR by competing with AhR for forming a heterodimer with Arnt and binding to the XRE sequence. Since the promoter region of mouse *AhRR* gene contains three copies of functional XREs, AhRR is inducible in an AhR-dependent manner [22,23]. These results indicate that AhR and AhRR form a regulatory feedback loop (Fig. 1). Other TCDD-responsive phase I (*CYP1A2, 1B1*) and phase II (*NADP(H):oxidoreductase, GST-Ya, UDP-glucronosyltransferase*) XMEs are also induced by the same mechanism as *CYP1A1* genes.

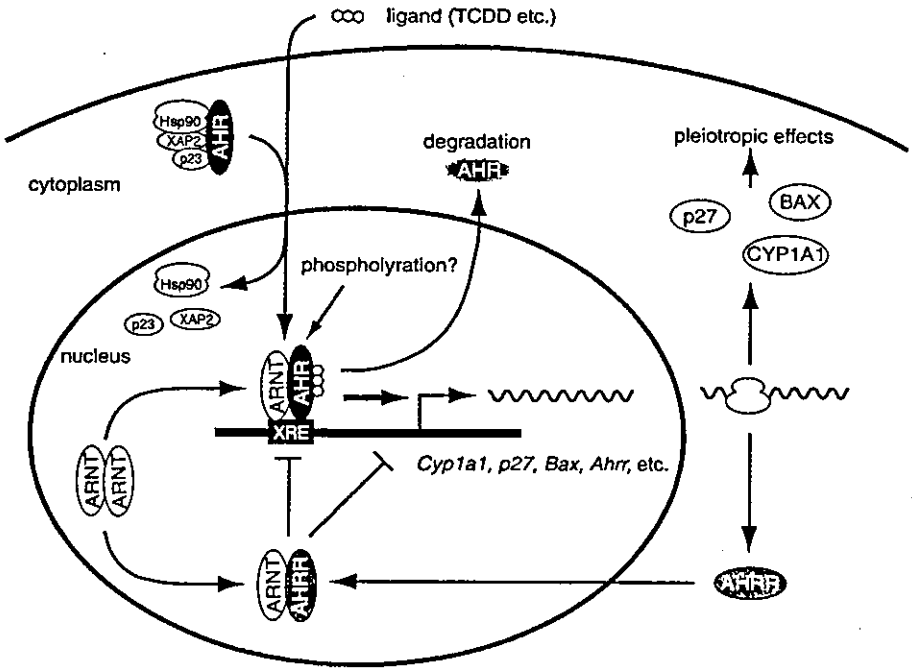

Fig. 1. Mechanisms of transcriptional activation by AhR and negative feedback regulation of AhR by AhRR. See text for a detailed discussion.

3. Molecular anatomy of AhR, AhRR and Arnt

AhR, AhRR and their common partner molecule, Arnt, are members of a structurally related gene family with characteristic structural motifs designated as bHLH (basic helix–loop–helix) and PAS (Per, Arnt/AhR, Sim homology) (Fig. 2) [24,25]. In the very NH_2-terminal region, these proteins contain a bHLH motif, which is shared by other transcription factors such as Myc and MyoD, and involved in DNA binding and hetero- or homodimerization. The sequence consisting of about 250 amino acids adjacent to the COOH-terminus of the bHLH region constitutes the PAS domain, which was initially identified as a conserved sequence among *Drosophila* PER, human ARNT and *Drosophila* SIM. The PAS domain contains two imperfect repeats of 50 amino acids, PAS A and PAS B, and is considered to function as an interactive surface for hetero- or homodimer formation. The PAS domain has recently been known to be distributed in a wide variety of proteins involved in circadian rhythm (PER, CLOCK, BMAL1), hypoxia response (HIF-1α, HIF-2α/HLF, HIF-3α), neurogenesis (SIM), and coactivation of transcription (SRC-1, TIF2) in the animal kingdom and is also found in bacterial proteins functioning as light and oxygen sensors [24,25]. The ligand binding domain of AhR is located in the sequence of 230–431 a.a. overlapping in part with the PAS B region, and also with the binding site for Hsp90 which keeps AhR structurally competent to bind a ligand [26]. In addition to PAS B region, Hsp90 interacts with the bHLH region to mask the nuclear localization signal (NLS) of AhR, resulting in the cytoplasmic maintenance of AhR. Ligand binding to AhR protein most probably changes the conformation of the Hsp90/AhR complex to expose the NLS of AhR, leading to nuclear translocation of the complex [27]. In addition, AhR contains a nuclear export signal (NES) in its second helix of the bHLH domain [28,29]. This NES is necessary for the nuclear export of the AhR protein followed by proteasome degradation [29]. Both NLS and NES sequences are also found in AhRR protein, but its functional significance has not yet been analyzed. Arnt contains an NLS in the NH_2-terminal region of the bHLH domain for constitutive nuclear localization [30]. A recent report has suggested that AhR contains LXCXE motif in the PAS B, which interacts with tumor suppressor Rb [31]. The transactivation activity is distributed broadly in the COOH-terminal half of the AhR molecule, while that of Arnt is limited to the very COOH-terminal 43 a.a. sequence [32]. As described above, the transactivation activity of the AhR/Arnt transactivation domains are mediated through CBP/p300 and RIP140 coactivators. Beyond the PAS A domain, the COOH-terminal half of AhRR differs greatly from that of AhR and function as a transcriptional repressor to the activity of AhR.

4. Vertebrate and invertebrate homologs of AhR, AhRR and Arnt

cDNAs of AhR homologs have been cloned from various species of animals ranging from mammals to flies and nematodes. Although only one AhR homolog has been identified in mammalian species despite extensive efforts, Hahn et al. [33] have reported cDNAs of two AhR homologs from *Fundulus heteroclitus* (FhAhR1 and FhAhR2). These two homologs of fish AhR mRNAs are derived from their independent genes. Rainbow trout also expresses at least two isoforms of AhR (rtAhR2α and rtAhR2β), although rtAhR1 has not yet been identified [34]. Interestingly, the expressions of rtAhR2α and rtAhR2β mRNAs are induced by TCDD, indicating that a positive autoregulatory mechanism of AhR may function in fish. Recently, fish AhRR counterpart has been reported [35]. This suggests that

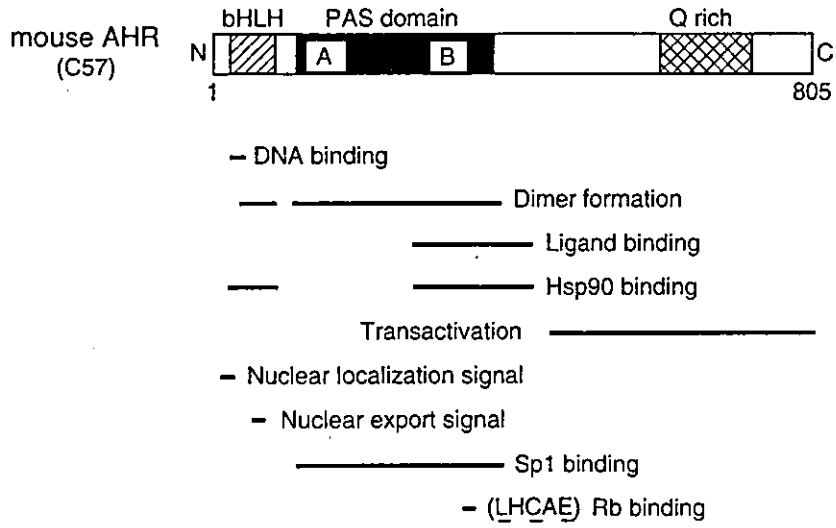

Fig. 2. Schematic representation of functional domain of AhR. (Hatched box) bHLH (basic helix–loop–helix); (closed box) PAS (Per–Arnt–Sim) domain; (A and B) PAS A and B repeats; (cross hatched box) Q-rich (glutamine rich) region; the location of functional domains are indicated by bars.

negative feedback regulation of AhR function by AhRR is conserved between mammal and fish.

For invertebrate species, AhR and Arnt homologs have been found in both *Drosophila* and *Caenorhabditis elegans* [36,37]. Spineless is an AhR homolog in *Drosophila*, and deletion of the *spineless* gene caused morphological transformation in distal legs and antennae of adult flies. Spineless forms a heterodimer with Tango (a *Drosophila* homolog of mammalian Arnt) and recognizes the same XRE sequence as mammalian AhR/Arnt heterodimer does. AHR-1 is the *C. elegans* homolog of AhR and forms a heterodimer with an Arnt homolog of *C. elegans*, AHA-1, which binds the XRE. However, it remains unknown whether or not these invertebrate AhR homologs can mediate the toxicological effects of xenobiotics including dioxin, because nematode AHR-1 appears to exhibit no ability of binding to β-naphthoflavone like the mammalian AhR [35]. These results suggest that a basic mechanism of the AhR/Arnt function is conserved between vertebrates and invertebrates, although their functions are not completely identical.

5. Target genes of AhR

As mentioned above, some phase I and phase II XMEs, and *AhRR* genes are the target genes of AhR and are induced in the presence of AhR ligands. In addition to these genes, a number of genes involved in cell proliferation (TGF-β, IL-1β and PAI-2), cell cycle regulation (p27 and jun-B), apoptosis (Bax), are known to be induced by AhR ligands [4–6,38,39]. Most of these genes are found to contain the XRE in their regulatory region, indicating that ligand-activated AhR upregulates the expression of these genes by directly bound to the XRE sequences (i.e. primary effects). On the other hand, indirect mechanisms (i.e. secondary effects) have been reported with the induction of multidrug resistance gene *mdr1* by 3-methylchoranthrene (3-MC) [40]. In this case, 3-MC induced XMEs in an AhR-dependent manner and the induced XMEs metabolically activated 3-MC to genotoxic metabolites that modify nucleotide bases of DNA. The modified DNA stabilizes p53, and the accumulated p53 in turn up-regulates the expression of *mdr1* gene by binding to its cognate DNA sequence in the promoter of *mdr1* gene. DNA microarray analysis has revealed that 310 genes were either up- or down-regulated in TCDD-treated HepG2 cells [41]. Of the 310 genes affected by TCDD, 108 genes could still exhibit the TCDD effects even by the simultaneous treatment with cycloheximide, a protein synthesis inhibitor, while the remaining 202 genes apparently lost the TCDD effects by cycloheximide. These results suggest that the expression of the former 108 genes is directly regulated by TCDD without protein synthesis, while the remaining 202 genes requires protein synthesis to show their regulated expression by TCDD. Safe et al. [42] have reported that the enhanced expression of cathepsin D and c-*fos* with estrogen treatment was inhibited in the presence of TCDD through the XRE sequence in the promoter of these genes. Although precise mechanisms of this inhibition still remain controversial, there is some possibility that AhR may play an inhibitory role in the transcription by binding to a specific sequence of XRE, designated inhibitory XRE. Recently, we have found that AhR up-regulated the expression of DNA polymerase κ, which replicates DNA in an error-prone manner. This result may explain why AhR is also involved in the promotion of chemical carcinogenesis [43].

6. Polymorphism in AhR gene

It is well known that there are marked strain and species differences in sensitivity to TCDD. LD_{50} value of TCDD varies over a 5000-fold range among different species of animals. For example, LD_{50} values vary from 1 μg/kg for guinea pig, the most sensitive animal, to >5000 μg/kg for hamster, the most resistant [7]. In mice, the difference in the responsiveness to TCDD among strains depends on the *AhR* alleles. cDNA cloning of a high-responder (C57BL) and low-responder (DBA) mice revealed that Ala-to-Val sub-

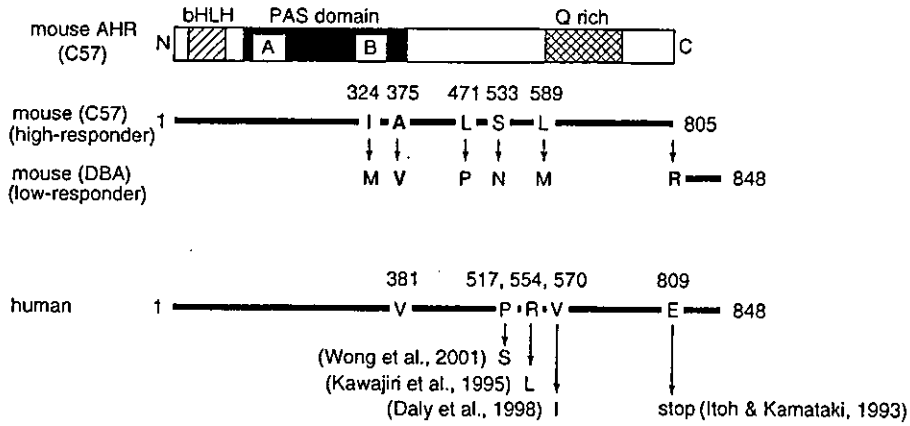

Fig. 3. Polymorphic forms of mouse and human AhRs. Amino acid replacements for high responder (C57BL/6), low responder (DBA/2) mice and human AhR are indicated. The bold Ala and Val residues are important for ligand binding in two strains of mice. See text for details.

stitution at codon 375 and the COOH-terminal extension in DBA mice reduced the binding affinity of AhR toward TCDD and, therefore, lowered the inducibility of XMEs (Fig. 3) [44]. Polymorphism in the *AhR* loci is also found in the rat [45]. TCDD-sensitive Long–Evans (L–E) (LD_{50}, 10–20 μg/kg) and insensitive Han/Wistar (H/W) (LD_{50}, >9600 μg/kg) rats show about 1000-fold difference in sensitivity. cDNA cloning revealed that AhR cDNA sequence of L–E rat is the same as that of Sprague–Dawley rat previously determined, while H/W rat AhR cDNA carries a point mutation in the first base of intron 10, resulting in a reading frameshift with a varied amino acid sequence of the COOH-terminal transactivation domain [45]. In human, three genetic variations in AhR gene have been reported [46–48]. Polymorphisms at $Lys^{554}Leu$, $Val^{570}Ile$ and $Pro^{571}Ser$ do not seem to be related to any phenotype of TCDD toxicity, if they occur independently. On the other hand, Wong et al. [48] reported that the combination of $Lys^{554}Leu$ and $Val^{570}Ile$ mutations abrogate *CYP1A1* induction in the transient transfection experiment. This result indicates a possibility that individual genetic variations in the *AhR* gene affect the TCDD-inducible toxicity in human.

7. AhR-deficient mice

AhR-null mice were generated by three independent groups [8,49,50]. AhR-null mice were born in normal Mendelian genetics, indicating no embryonic lethality of AhR-null mice. However, growth rate of the AhR-null mice was significantly retarded as compared with the wild type mice for the first 3 weeks of life, and the mutant mice were revealed to be defective in development of liver and immune system [50]. Several phenotypic defects have been reported for adult AhR-null mice, such as retinoid accumulation in liver and abnormal hepatic and kidney vascular structures [51,52]. It has also been reported that female AhR-null mice had difficulty in maintaining conception, lactation, and rearing pups to weaning [53]. Concerning xenobiotic metabolism, the lack of AhR abolished the inducible expression of *CYP1A1* and *1A2* genes in response to TCDD or PAHs and resulted in a loss of teratogenesis caused by TCDD and susceptibility to chemical carcinogenesis by benzo[a]pyrene [8,10]. Although the genes responsible for TCDD-induced teratogenesis remain to be identified, the loss of inducibility in expression of *CYP1A1*, *1A2* and *1B1*, which metabolically activate various procarcinogens to ultimate carcinogens, is considered to be a cause of resistance to chemical carcinogenesis in AhR-null mice.

8. Agonists and antagonists for AhR

It is well known that TCDD is the most potent ligand of AhR with an extremely low K_d value. Other types of halogenated aromatic hydrocarbons such as PCB and PAHs such as benzo[a]pyrene also function as ligand to AhR. Some flavonoids play an antagonistic or agonistic role for AhR [54,55]. It has been reported that 7-ketocholesterol functions as an AhR antagonist and actually antagonizes the TCDD effects in vivo [56]. This antagonistic effect of 7-ketocholesterol has been suggested to have physiological significance because it was observed at its physiological plasma concentration in human blood. Resveratrol, a plant steroid, was also reported to be an antagonist for AhR [57]. It has been an interesting and long-standing problem to find a true and intrinsic ligand of AhR. Recently, a number of endogenous AhR ligands have been reported to have a high affinity toward AhR [58,59]. Most of these chemicals are tryptophan derivatives. UV-irradiated or ozone-treated tryptophan products function as an AhR agonist. Some of the purified products were reported to function as a potent ligand of AhR. Indirubin and indigo isolated from urine were reported to serve as an even more potent ligand of AhR than TCDD in a yeast assay system [60].

9. Conclusion

A number of studies have revealed precise mechanisms of *CYP1A1* induction by dioxin and other aromatic hydrocarbons. Ligand-activated AhR directly enhance the *CYP1A1* gene expression by binding to the XRE in the promoter region. Although it is true that AhR is one of the xenobiotic receptors, recent studies of AhR-null mice have suggested that AhR plays a regulatory role in homeostasis and development of animals in addition to XMEs induction, suggesting the presence of an intrinsic ligand to AhR. Although a number of putative intrinsic AhR ligands have been reported, it would be difficult to identify true intrinsic ligands of AhR, until the intrinsic roles of AhR other than gene regulation of a series of XMEs are clarified.

Acknowledgements

This work was supported in part by a Grant-in-aid for scientific research on priority area (A) from the Ministry of Education, Culture, Sports, Science and Technology, Japan, and grants from the Core Research for Evolutional Science and Technology (CREST), Japan Science and Technology Corporation, from Sankyo Co., and from Research for the Future Program of the Japan Society for the Promotion Science.

References

[1] D.W. Nebert, F.J. Gonzalez, Annu. Rev. Biochem. 56 (1987) 945–993.
[2] D.W. Nebert, A.L. Roe, M.Z. Dieter, W.A. Solis, Y. Yang, T.P. Dalton, Biochem. Pharmacol. 59 (2000) 65–85.
[3] D.J. Waxman, Arch. Biochem. Biophys. 369 (1999) 11–23.

[4] O. Hankinson, Annu. Rev. Pharmacol. Toxicol. 35 (1995) 307–340.
[5] K. Sogawa, Y. Fujii-Kuriyama, J. Biochem. (Tokyo) 122 (1997) 1075–1079.
[6] M.E. Hahn, Comp. Biochem. Physiol., Part C Pharmacol. Toxicol. Endocrinol. 121 (1998) 23–53.
[7] A. Poland, J.C. Knutson, Annu. Rev. Pharmacol. Toxicol. 22 (1982) 517–554.
[8] J. Mimura, K. Yamashita, K. Nakamura, M. Morita, T.N. Takagi, K. Nakao, M. Ema, K. Sogawa, M. Yasuda, M. Katsuki, Y. Fujii-Kuriyama, Genes Cells 2 (1997) 645–654.
[9] P.M. Fernandez-Salguero, J.M. Ward, J.P. Sundberg, F.J. Gonzalez, Vet. Pathol. 34 (1997) 605–614.
[10] Y. Shimizu, Y. Nakatsuru, M. Ichinose, Y. Takahashi, H. Kume, J. Mimura, Y. Fujii-Kuriyama, T. Ishikawa, Proc. Natl. Acad. Sci. U. S. A. 97 (2000) 779–782.
[11] A. Fujisawa-Sehara, K. Sogawa, M. Yamane, Y. Fujii-Kuriyama, Nucleic Acids Res. 15 (1987) 4179–4191.
[12] B.K. Meyer, M.G. Pray-Grant, J.P. Vanden Heuvel, G.H. Perdew, Mol. Cell. Biol. 18 (1998) 978–988.
[13] B.K. Meyer, G.H. Perdew, Biochemistry 38 (1999) 8907–8917.
[14] A. Kazlauskas, L. Poellinger, I. Pongratz, J. Biol. Chem. 274 (1999) 13519–13524.
[15] H.P. Ko, S.T. Okino, Q. Ma , J.P. Whitlock Jr., Mol. Cell. Biol. 16 (1996) 430–436.
[16] A. Kobayashi, K. Sogawa, Y. Fujii-Kuriyama, J. Biol. Chem. 271 (1996) 12310–12316.
[17] A. Kobayashi, K. Numayama-Tsuruta, K. Sogawa, Y. Fujii-Kuriyama, J. Biochem. 122 (1997) 703–710.
[18] M.B. Kumar, R.W. Tarpey, G.H. Perdew, J. Biol. Chem. 274 (1999) 22155–22164.
[19] M.B. Kumar, G.H. Perdew, Gene Expr. 8 (1999) 273–286.
[20] S. Park, E.C. Henry, T.A. Gasiewicz, Arch. Biochem. Biophys. 381 (2000) 302–312.
[21] S.L. Levine, G.H. Perdew, Mol. Pharmacol. 59 (2001) 557–566.
[22] J. Mimura, M. Ema, K. Sogawa, Y. Fujii-Kuriyama, Genes Dev. 13 (1999) 20–25.
[23] T. Baba, J. Mimura, K. Gradin, A. Kuroiwa, T. Watanabe, Y. Matsuda, J. Inazawa, K. Sogawa, Y. Fujii-Kuriyama, J. Biol. Chem. 276 (2001) 33101–33110.
[24] Y.Z. Gu, J.B. Hogenesch, C.A. Bradfield, Annu. Rev. Pharmacol. Toxicol. 40 (2000) 519–561.
[25] B.L. Taylor, I.B. Zhulin, Microbiol. Mol. Biol. Rev. 63 (1999) 479–506.
[26] P. Coumailleau, L. Poellinger, J.A. Gustafsson, M.L. Whitelaw, J. Biol. Chem. 270 (1995) 25291–25300.
[27] M.J. Lees, M.L. Whitelaw, Mol. Cell. Biol. 19 (1999) 5811–5822.
[28] T. Ikuta, H. Eguchi, T. Tachibana, Y. Yoneda, K. Kawajiri, J. Biol. Chem. 273 (1998) 2895–2904.
[29] N.A. Davarinos, R.S. Pollenz, J. Biol. Chem. 274 (1999) 28708–28715.
[30] H. Eguchi, T. Ikuta, T. Tachibana, Y. Yoneda, K. Kawajiri, J. Biol. Chem. 272 (1997) 17640–17647.
[31] N.L. Ge, C.J. Elferink, J. Biol. Chem. 273 (1998) 22708–22713.
[32] K. Sogawa, K. Iwabuchi, H. Abe, Y. Fujii-Kuriyama, J. Cancer Res. Clin. Oncol. 121 (1995) 612–620.
[33] M.E. Hahn, S.I. Karchner, M.A. Shapiro, S.A. Perera, Proc. Natl. Acad. Sci. U. S. A. 94 (1997) 13743–13748.
[34] C.C. Abnet, R.L. Tanguay, M.E. Hahn, W. Heideman, R.E. Peterson, J. Biol. Chem. 274 (1999) 15159–15166.
[35] S.I. Karchner, D.G. Franks, W.H. Powell, M.E. Hahn, J. Biol. Chem. 277 (2002) 6949–6959.
[36] D.M. Duncan, E.A. Burgess, I. Duncan, Genes Dev. 12 (1998) 1290–1303.
[37] J.A. Powell-Coffman, C.A. Bradfield, W.B. Wood, Proc. Natl. Acad. Sci. U. S. A. 95 (1998) 2844–2849.
[38] S.K. Kolluri, C. Weiss, A. Koff, M. Gottlicher, Genes Dev. 13 (1999) 1742–1753.
[39] T. Matikainen, G.I. Perez, A. Jurisicova, J.K. Pru, J.J. Schlezinger, H.Y. Ryu, J. Laine, T. Sakai, S.J. Korsmeyer, R.F. Casper, D.H. Sherr, J.L. Tilly, Nat. Genet. 28 (2001) 355–360.
[40] M.C. Mathieu, I. Lapierre, K. Brault, M. Raymond, J. Biol. Chem. 276 (2001) 4819–4827.
[41] F.W. Frueh, K.C. Hayashibara, P.O. Brown , J.P. Whitlock Jr., Toxicol. Lett. 122 (2001) 189–203.
[42] S. Safe, F. Wang, W. Porter, R. Duan, A. McDougal, Toxicol. Lett. 102–103 (1998) 343–347.
[43] T. Ogi, J. Mimura, M. Hikida, H. Fujimoto, Y. Fujii-Kuriyama, H. Ohmori, Genes Cells 6 (2001) 943–953.
[44] M. Ema, N. Ohe, M. Suzuki, J. Mimura, K. Sogawa, S. Ikawa, Y. Fujii-Kuriyama, J. Biol. Chem. 269 (1994) 27337–27343.
[45] R. Pohjanvirta, J.M.Y. Wong, W. Li, P.A. Harper, J. Tuomisto, A.B. Okey, Mol. Pharmacol. 54 (1998) 86–93.
[46] K. Kawajiri, J. Watanabe, H. Eguchi, K. Nakachi, C. Kiyohara, S. Hayashi, Pharmacogenetics 5 (1995) 151–158.
[47] J.M. Wong, P.A. Harper, U.A. Meyer, K.W. Bock, K. Morike, J. Lagueux, P. Ayotte, R.F. Tyndale, E.M. Sellers, D.K. Manchester, A.B. Okey, Pharmacogenetics 11 (2001) 85–94.
[48] J.M. Wong, A.B. Okey, P.A. Harper, Biochem. Biophys. Res. Commun. 288 (2001) 990–996.
[49] P. Fernandez-Salguero, T. Pineau, D.M. Hilbert, T. McPhail, S.S. Lee, S. Kimura, D.W. Nebert, S. Rudikoff, J.M. Ward, F.J. Gonzalez, Science 268 (1995) 722–726.
[50] J.V. Schmidt, G.H. Su, J.K. Reddy, M.C. Simon, C.A. Bradfield, Proc. Natl. Acad. Sci. U. S. A. 93 (1996) 6731–6736.
[51] F. Andreola, P.M. Fernandez-Salguero, M.V. Chiantore, M.P. Petkovich, F.J. Gonzalez, L.M. De Luca, Cancer Res. 57 (1997) 2835–2838.
[52] G.P. Lahvis, S.L. Lindell, R.S. Thomas, R.S. McCuskey, C. Murphy, E. Glover, M. Bentz, J. Southard, C.A. Bradfield, Proc. Natl. Acad. Sci. U. S. A. 97 (2000) 10442–10447.
[53] B.D. Abbott, J.E. Schmid, J.A. Pitt, A.R. Buckalew, C.R. Wood, G.A. Held, J.J. Diliberto, Toxicol. Appl. Pharmacol. 155 (1999) 62–70.
[54] J.J. Reiners Jr., R. Clift, P. Mathieu, Carcinogenesis 20 (1999) 1561–1566.
[55] H. Ashida, I. Fukuda, T. Yamashita, K. Kanazawa, FEBS Lett. 476 (2000) 213–217.
[56] J.F. Savouret, M. Antenos, M. Quesne, J. Xu, E. Milgrom, R.F. Casper, J. Biol. Chem. 276 (2001) 3054–3059.
[57] R.F. Casper, M. Quesne, I.M. Rogers, T. Shirota, A. Jolivet, E. Milgrom, J.F. Savouret, Mol. Pharmacol. 56 (1999) 784–790.
[58] S. Heath-Pagliuso, W.J. Rogers, K. Tullis, S.D. Seidel, P.H. Cenijn, A. Brouwer, M.S. Denison, Biochemistry 37 (1998) 11508–11515.
[59] Y.D. Wei, L. Bergander, U. Rannug, A. Rannug, Arch. Biochem. Biophys. 383 (2000) 99–107.
[60] J. Adachi, Y. Mori, S. Matsui, H. Takigami, J. Fujino, H. Kitagawa, C.A. Miller III, T. Kato, K. Saeki, T. Matsuda, J. Biol. Chem. 276 (2001) 31475–31478.

Short Communication

Aryl Hydrocarbon Hydroxylase Represents CYP1B1, and not CYP1A1, in Human Freshly Isolated White Cells: Trimodal Distribution of Japanese Population According to Induction of CYP1B1 mRNA by Environmental Dioxins[1]

Kenji Toide, Hiroshi Yamazaki, Rikako Nagashima, Keisuke Itoh, Shunsuke Iwano, Yoshiki Takahashi, Shaw Watanabe, and Tetsuya Kamataki[2]

Graduate School of Pharmaceutical Sciences, Hokkaido University, Sapporo 060-0812 [K. T., H. Y., R. N., K. I., S. I., Y. T., T. K.] and Faculty of Applied Bioscience, Tokyo University of Agriculture, Tokyo 156-8502 [S. W.], Japan

Abstract

The expression level of mRNAs for cytochrome P450 (CYP) 1A1 and 1B1 in freshly prepared white cells from 72 subjects exposed to dioxins at waste incinerators was investigated. The amounts of CYP1B1 mRNA ranged from 0.16 to 671 molecules/10^7 molecules of 18S rRNA, whereas the amounts of CYP1A1 mRNA were <6 molecules/10 ng total RNA, indicating that CYP1A1 was not induced to a detectable level by environmentally exposed dioxins. The inducibility of CYP1B1 mRNA in leukocytes, defined as the ratio of CYP1B1 mRNA to the plasma concentration of dioxins, varied among the subjects. It was found that the subjects showed trimodal distribution according to inducibility: 39 (54.2%), 25 (34.7%), and 8 (11.1%) of 72 subjects were judged as poor, intermediate, and high responders to environmental dioxins, respectively. The amounts of CYP1B1 mRNA in leukocytes of the intermediate and high responders were highly correlated with the plasma concentrations of dioxins ($P < 0.05$ and <0.01). These results suggest that CYP1B1 with polymorphic inducibility by dioxins is involved in aromatic hydrocarbon hydroxylase activities in human lymphocytes.

Introduction

Carcinogenic PAHs[3] are metabolically activated by enzymes to generate reactive intermediates capable of binding to DNA to cause the mutation of cancer-related genes (1, 2). Thus, the capacity of enzymes responsible for the activation of the carcinogenic PAHs has been regarded as one of the factors affecting the risk to chemical carcinogenesis. Kellermann *et al.* (3) first reported that the capacity of individuals to induce AHH in lymphocytes in response to PAH was apparently associated with the individual differences in the risk of bronchogenic carcinoma, suggesting that the amount of AHH was one of the key determinants of the cancer risk. After this result, Guirgis *et al.* (4) and Trell *et al.* (5) reported that AHH activity in individuals correlated well with the risk of lung cancer and laryngeal carcinoma. The original assay of Kellermann *et al.* (3) was to measure PAH-inducible AHH activity in mitogen-activated lymphoblasts cultured for 96 h.

CYP1A1 had been thought to be a sole enzyme acting as AHH until the role of CYP1B1 in the metabolic activation of PAHs was discovered (6, 7). The role of CYP1B1 in the metabolic activation of chemical carcinogens was found during the course of studies on the responsiveness to 2,3,7,8-tetrachlorodibenzo-*p*-dioxin (8). Thus, it seemed interesting to determine whether the AHH activity in the lymphoblast cultures prepared by the method of Kellermann *et al.* (3) was attributable to CYP1A1 or CYP1B1.

We initiated this study to determine whether either one or both mRNAs for CYP1A1 and CYP1B1 were induced in human leukocytes in response to environmental dioxins in Japanese incinerator workers. We found that CYP1B1 mRNA, but not CYP1A1 mRNA, was detectable in essentially all subjects and that there were individual variations in the responsiveness to environmental dioxins to induce CYP1B1 mRNA.

Materials and Methods

Human Blood Samples. Blood samples used in this study were taken from Japanese subjects who were occupationally exposed to dioxins at waste incinerators. The concentrations of dioxins (pg TEQ/g lipid), which were defined as the sum of polychlorinated dibenzo-*p*-dioxins normalized with a WHO toxic equivalent factor, were determined by gas chromatography high-resolution mass spectrometry as described previously (9). This study was approved by the ethics committee of Hokkaido University.

First-strand cDNA Synthesis. Total RNAs in human leukocytes were isolated by a TRIzol LS reagent system (Invitrogen, Carlsbad, CA). Nothing was done to separate the different white cell types. First-strand cDNA was then synthesized. Reverse transcriptase reaction was performed under the following conditions: a reaction mixture contained 50 mM Tris-HCl (pH 8.3), 75 mM KCl, 3 mM $MgCl_2$, 10 mM DTT, 0.5 mM each deoxynucleotide triphosphate, 10 ng/μl total RNA, 4.5 ng/μl random primer pd$(N)_6$ (Promega, Madison, WI), 2 units/μl a

Received 8/8/02; revised 1/3/03; accepted 1/9/03.
The costs of publication of this article were defrayed in part by the payment of page charges. This article must therefore be hereby marked *advertisement* in accordance with 18 U.S.C. Section 1734 solely to indicate this fact.
[1] Supported in part by Grant-in-Aid 99-2 from The Organization for Pharmaceutical Safety and Research; Ministry of Education, Culture, Sports, Science and Technology of Japan; Ministry of Health, Labour and Welfare of Japan and Core Research for Evolutional Science and Technology.
[2] To whom requests for reprints should be addressed, at Laboratory of Drug Metabolism, Graduate School of Pharmaceutical Sciences, Hokkaido University N12W6, Kita-ku, Sapporo 060-0812, Japan. Fax: 81-11-706-4978; E-mail: kamataki@pharm.hokudai.ac.jp.
[3] The abbreviations used are: PAH, polycyclic aromatic hydrocarbon; AHH, aromatic hydrocarbon hydroxylase; CYP, cytochrome P450; TEQ, toxic equivalents to 2,3,7,8-tetrachlorodibenzo-*p*-dioxin.

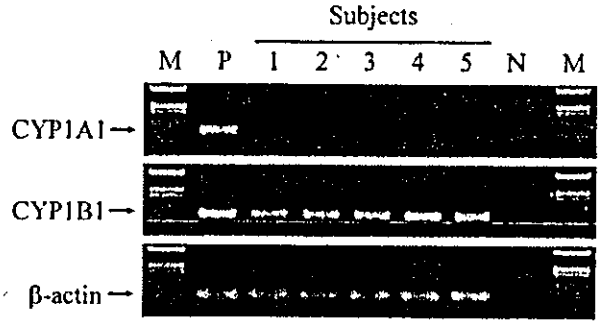

Fig. 1. Expression of CYP1A1 and CYP1B1 mRNA in total RNA prepared from 5 subjects who might be highly disclosed to dioxins. An amplified fragment size for CYP1A1, CYP1B1, or β-actin is 139, 139, or 78 bp, respectively. *M*, DNA size marker; *N*, none template control; *P*, positive control.

Maloney murine leukemia virus reverse transcriptase (Promega), and 0.4 units/μl RNase inhibitor (Toyobo, Osaka, Japan). The mixtures were treated at 25°C for 10 min and then 37°C for 60 min.

PCR Condition. Primers used for the amplification of cDNAs for CYP1A1 and CYP1B1 were CYP1A1-RTF, 5′-ccttcatcctggagaccttcc-3′; CYP1A1-RTR, 5′-atggttgatctgccactggttt-3′; CYP1B1-RTF, 5′-agaacgtaccggccactatc-3′; and CYP1B1-RTR, 5′-cacgacctgatccaattctg-3′. A quantitative PCR to determine the amount of CYP1B1 mRNA was performed in a real-time PCR machine, LightCycler (Roche Diagnostics, Mannheim, Germany), using a LightCycler-FastStart DNA Master SYBR Green I (Roche Diagnostics) according to the manufacturer's instructions. PCR amplifications were performed in 40 cycles with melting at 95°C for 15 s, annealing at 60°C for 5 s, and extension at 72°C for 7 s. The amounts of 18S rRNA used as an internal standard were determined by a TaqMan Ribosomal RNA Control Reagents VIC Probe (Applied Biosystems, Foster City, CA). PCR conditions for amplification of β-actin mRNA were as described previously (10).

Results

Expression of mRNAs for CYP1A1 and CYP1B1. The expression of mRNAs for CYP1A1 and CYP1B1 in leukocytes from 72 subjects was quantified with reverse transcription-PCR. Although the expression of CYP1B1 mRNA and β-actin mRNA was detectable in all subjects, the expression of CYP1A1 mRNA could not be seen under present experimental conditions (Fig. 1). We could not detect the expression of CYP1A1 mRNA in all subjects with either ABI 7700 (Applied Biosystems) or TaqMan probe (Applied Biosystems) in addition to the real-time PCR, with a detection limit of CYP1A1 mRNA as low as 6 molecules/10 ng total RNA (data not shown).

Inducibility of the *CYP1B1* Gene. The expression level of CYP1B1 mRNA in human leukocytes was quantified with the quantitative reverse transcription-PCR. The amounts of CYP1B1 mRNA are shown as the copy number of CYP1B1 mRNA/10^7 molecules of 18S rRNA. As shown in Fig. 2*A*, the amounts of CYP1B1 mRNA in total RNAs prepared from 72 human leukocytes ranged from 0.18 to 671 molecules/10^7 molecules of 18S rRNA. The ratio of the amounts of CYP1B1 mRNA to the concentration of dioxins in plasma was defined as the inducibility of CYP1B1 mRNA. The ratio varied over three orders of magnitude. The probit plot analysis for the distribution of the inducibility of CYP1B1 mRNA is shown in Fig. 2*B*. The results indicate the trimodal distribution of subjects according to the inducibility of CYP1B1 mRNA. Thus, low, intermediate, and high inducibility groups consisted of 39 (54.2%), 25 (34.7%), and 8 (11.1%) subjects, respectively.

Correlation between the Amounts of CYP1B1 mRNA and Concentrations of Dioxins. To determine whether a correlation was seen between the amounts of CYP1B1 mRNA and concentrations of dioxins, least squared regression analysis was performed in high, intermediate, and low inducibility subjects, respectively (Fig. 3). The amounts of CYP1B1 mRNA significantly correlated with the concentrations of dioxins in the high inducibility group ($n = 8$, $r = 0.86$, $P < 0.01$). A low but significant correlation coefficient was also observed in the intermediate inducibility group ($n = 25$, $r = 0.41$, $P < 0.05$). There was no correlation in the low group.

Discussion

The *CYP1A1* and *CYP1B1* genes are members of aromatic hydrocarbon receptor battery genes. The expression of these genes, therefore, is thought to be induced concomitantly through the activation of aromatic hydrocarbon receptor. In agreement with this concept, both CYP1A1 and CYP1B1 mRNAs were induced by the treatment of human blood monocytes with dioxins or PAHs *in vitro* (11, 12). The subjects whose leukocytes were analyzed in this study were workers occupationally exposed to dioxins at waste incinerators (9). Thus, we expected that both CYP1A1 and CYP1B1 mRNAs might be induced by environmental exposure to dioxins. However, we found that the expression of only CYP1B1 mRNA was induced, whereas the expression of CYP1A1 mRNA was not induced. The reason accounting for the fact that only CYP1B1 mRNA was induced is not known at present.

After the first report on the significant association between AHH inducibility in human lymphocytes and the bronchogenic cancer risk (3), many papers have appeared to argue that the apparent association was not seen between the AHH inducibility and susceptibility to lung cancer or other cancers (13–17). The reason for this apparent discrepancy has been partly accounted for by the difficulty of the measurement and the seasonal variation of the AHH activity in human lymphocytes (18, 19). It has long been believed that CYP1A1 is the major isoform involved in AHH activities in human lymphocytes (7). Recent reports have indicated that both human CYP1A1 and CYP1B1 are involved in the AHH activities (7, 8, 20). In addition, CYP1B1 is reported to exist as the major CYP isoform in human blood monocytes (11). Although there is a fundamental difference between AHH activities in the cultured mitogen-activated lymphoblasts reported previously (3–5) and the mRNA levels in the freshly isolated leukocytes in this study, together with the data presented herein, it may be reasonable to assume that CYP1B1 rather than CYP1A1 is responsible for the AHH activity in human lymphocytes *in vivo*. Additional experiments still need to be done in this context.

A trimodal distribution of subjects according to the inducibility of AHH activity in human lymphocytes was reported in a previous report, which was apparently associated with the cancer risk (3). In agreement with the previous report, we found a similar trimodal distribution in the inducibility of CYP1B1 mRNA based on the calculated ratio of the amounts of CYP1B1 mRNA to the concentrations of dioxins in plasma (Fig. 2*B*), lending further support to the idea that CYP1B1 rather than CYP1A1 is likely to be a major CYP isoform involved in AHH activity in human lymphocytes. The polymorphic inducibility

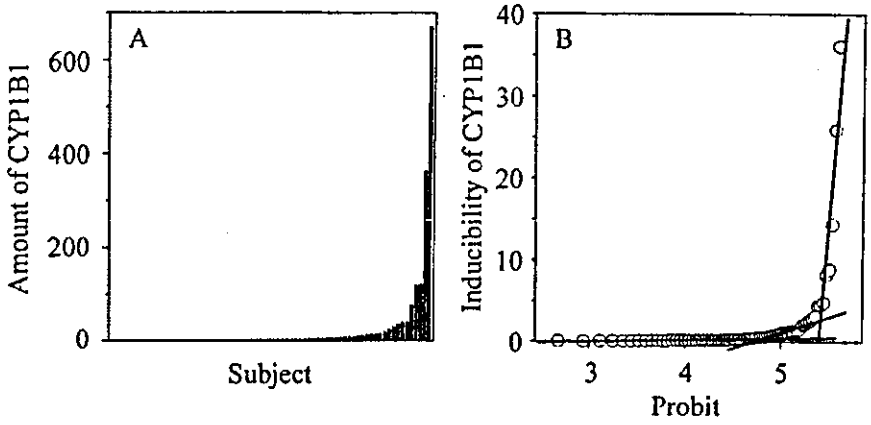

Fig. 2. *A*, the amount of CYP1B1 mRNA in human blood. The amount of CYP1B1 mRNA represents copy number of CYP1B1 mRNA/10^7 copies of 18S rRNA (molecules/10^7 molecules of 18S rRNA). *B*, probit plot for the distribution of CYP1B1 mRNA inducibility in human leukocytes. The ratio between the amount of CYP1B1 mRNA (molecules/10^7 molecules of 18S rRNA) and concentration of dioxins (pg TEQ/g lipid) was defined as the inducibility of CYP1B1.

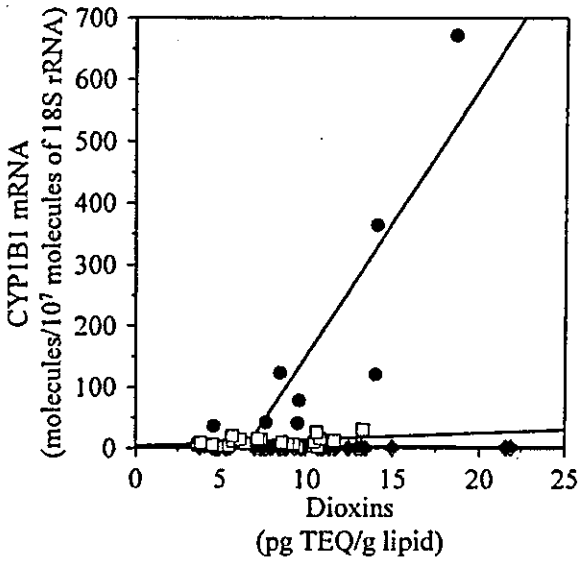

Fig. 3. The correlation between the amount of CYP1B1 mRNA and dioxins concentration in each inducibility group. A significant correlation was observed in intermediate ($r = 0.412$, $P = 0.041$) or high inducibility group ($r = 0.861$, $P = 0.006$), respectively.

in CYP1B1 mRNA has been observed *in vitro* (12). The mechanism(s) responsible for the polymorphic inducibility of CYP1B1 mRNA in human lymphocytes is still unclear at present. However, according to the previous concept (3–5), it may be possible to assume that the high inducibility subjects have higher risk to cancers caused by environmental carcinogens, such as PAHs.

The correlation between the amounts of CYP1B1 mRNA and concentration of dioxins was observed in both intermediate ($P < 0.05$) and high inducibility groups ($P < 0.01$; Fig. 3). The results also suggest an apparent threshold of dioxin concentration for the induction of CYP1B1 mRNA in human leukocytes. This threshold was calculated to be 6.5 pg TEQ/g lipid. This is the first to demonstrate the apparent threshold of the concentration of dioxins showing an influence in humans *in vivo*.

In conclusion, no expression of CYP1A1 mRNA and the polymorphic expression of CYP1B1 mRNA were observed in human leukocytes prepared from 72 subjects exposed to dioxins. The inducibility of CYP1B1 mRNA defined as the ratio of CYP1B1 mRNA to the plasma concentration of dioxins showed trimodal distribution similar to those of reported inducibility of AHH activity, suggesting that CYP1B1 is the major isoform involved in AHH activity in human lymphocytes.

References

1. Wood, A. W., Goode, R. L., Chang, R. L., Levin, W., Conney, A. H., Yagi, H., Dansette, P. M., and Jerina, D. M. Mutagenic and cytotoxic activity of benzo[*a*]pyrene 4, 5-, 7, 8-, and 9, 10-oxides and the six corresponding phenols. Proc. Natl. Acad. Sci. USA, *72:* 3176–3180, 1975.

2. Yang, S. K., McCourt, D. W., Leutz, J. C., and Gelboin, H. V. Benzo[*a*]pyrene diol epoxides: mechanism of enzymatic formation and optically active intermediates. Science (Wash. DC), *196:* 1199–1201, 1977.

3. Kellermann, G., Shaw, C. R., and Luyten-Kellermann. M. Aryl hydrocarbon hydroxylase inducibility and bronchogenic carcinoma. N. Engl. J. Med., *289:* 934–937, 1973.

4. Guirgis, H. A., Lynch, H. T., Mate, T., Harris, R. E., Wells, I., Caha, L., Anderson, J., Maloney, K., and Rankin, L. Aryl-hydrocarbon hydroxylase activity in lymphocytes from lung cancer patients and normal controls. Oncology, *33:* 105–109, 1976.

5. Trell, E., Korsgaard, R., Hood, B., Kitzing, P., Nordén, G., and Simonsson, B. G. Aryl hydrocarbon hydroxylase inducibility and laryngeal carcinomas. Lancet, *2:* 140, 1976.

6. Nebert, D. W., Puga, A., and Vasiliou, V. Role of the Ah receptor and the dioxin-inducible [*Ah*] gene battery in toxicity, cancer, and signal transduction. Ann. N. Y. Acad. Sci., *685:* 624–640, 1993.

7. Jaiswal, A. K., Gonzalez, F. J., and Nebert, D. W. Human P_1-*450* gene sequence and correlation of mRNA with genetic differences in benzo[a]pyrene metabolism. Nucleic Acids Res., *13:* 4503–4520, 1985.

8. Sutter, T. R., Tang, Y. M., Hayes, C. L., Wo, Y-Y. P., Jabs, E. W., Li, X., Yin, H., Cody, C. W., and Greenlee, W. F. Complete cDNA sequence of a human dioxin-inducible mRNA identifies a new gene subfamily of cytochrome P450 that maps to chromosome 2. J. Biol. Chem., *269:* 13092–13099, 1994.

9. Kitamura, K., Kikuchi, Y., Watanabe, S., Waechter, G., Sakurai, H., and Takada, T. Health effects of chronic exposure to polychlorinated dibenzo-*p*-dioxins (PCDD), dibenzofurans (PCDF) and coplanar PCB (Co-PCB) of municipal waste incinerator workers. J. Epidemiol., *10:* 262–270, 2000.

10. Toide, K., Takahashi, Y., Yamazaki, H., Terauchi, Y., Fujii, T., Parkinson, A., and Kamataki, T. Hepatocyte nuclear factor-1α is a causal factor responsible for interindividual differences in the expression of UDP-glucuronosyltransferase 2B7 mRNA in human livers. Drug Metab. Dispos., *30:* 613–615, 2002.

11. Baron, J. M., Zwadlo-Klarwasser, G., Jugert, F., Hamann, W., Rubben, A., Mukhtar, H., and Merk, H. F. Cytochrome P450 1B1: a major P450 isoenzyme in human blood monocytes and macrophage subsets. Biochem. Pharmacol., *56:* 1105–1110, 1998.

12. Spencer, D. L., Masten, S. A., Lanier, K. M., Yang, X., Grassman, J. A., Miller, C. R., Sutter, T. R., Lucier, G. W., and Walker, N. J. Quantitative analysis of constitutive and 2, 3, 7, 8-tetrachlorodibenzo-*p*-dioxin-induced cytochrome P450 1B1 expression in human lymphocytes. Cancer Epidemiol. Biomark. Prev., *8:* 139–146, 1999.

13. Paigen, B., Minowada, J., Gurtoo, H. L., Paigen, K., Parker, N. B., Ward, E., Hayner, N. T., Bross, I. D., Bock, F., and Vincent, R. Distribution of aryl

hydrocarbon hydroxylase inducibility in cultured human lymphocytes. Cancer Res., *37:* 1829–1837, 1977.

14. Paigen, B., Gurtoo, H. L., Minowada, J., Houten, L., Vincent, R., Paigen, K., Parker, N. B., Ward, E., and Hayner, N. T. Questionable relation of aryl hydrocarbon hydroxylase to lung-cancer risk. N. Engl. J. Med., *297:* 346–350, 1977.

15. Ward, E., Paigen, B., Steenland, K., Vincent, R., Minowada, J., Gurtoo, H. L., Sartori, P., and Havens, M. B. Aryl hydrocarbon hydroxylase in persons with lung or laryngeal cancer. Int. J. Cancer, *22:* 384–389, 1978.

16. Lieberman, J. Aryl hydrocarbon hydroxylase in bronchogenic carcinoma. N. Engl. J. Med., *298:* 686–687, 1978.

17. Kärki, N. T., Pokela, R., Nuutinen, L., and Pelkonen, O. Aryl hydrocarbon hydroxylase in lymphocytes and lung tissue from lung cancer patients and controls. Int. J. Cancer, *39:* 565–570, 1987.

18. Paigen, B., Ward, E., Reilly, A., Houten, L., Gurtoo, H. L., Minowada, J., Steenland, K., Havens, M. B., and Sartori, P. Seasonal variation of aryl hydrocarbon hydroxylase activity in human lymphocytes. Cancer Res., *41:* 2757–2761, 1981.

19. Kiyohara, C., Nakanishi, Y., Inutsuka, S., Takayama, K., Hara, N., Motohiro, A., Tanaka, K., Kono, S., and Hirohata, T. The relationship between CYP1A1 aryl hydrocarbon hydroxylase activity and lung cancer in a Japanese population. Pharmacogenetics, *8:* 315–323, 1998.

20. Shimada, T., Gillam, E. M., Sutter, T. R., Strickland, P. T., Guengerich, F. P., and Yamazaki, H. Oxidation of xenobiotics by recombinant human cytochrome P450 1B1. Drug Metab. Dispos., *25:* 617–622, 1997.

TOXICOLOGICAL SCIENCES 72, 235–241 (2003)
DOI: 10.1093/toxsci/kfg025

Effects of Polychlorinated Biphenyls, Kanechlor-500, on Serum Thyroid Hormone Levels in Rats and Mice

Yoshihisa Kato,*[,1] Koichi Haraguchi,† Tomoaki Yamazaki,* Yuriko Ito,* Shoji Miyajima,* Kiyomitsu Nemoto,* Nobuyuki Koga,§ Ryohei Kimura,* and Masakuni Degawa*

*School of Pharmaceutical Sciences, University of Shizuoka, 52–1, Yada, Shizuoka 422-8526, Japan; †Daiichi College of Pharmaceutical Sciences, 22–1, Tamagawa-cho, Minami-ku, Fukuoka 815-8511, Japan; and §Faculty of Nutritional Sciences, Nakamura Gakuen University, 5–7–1 Befu, Johnan-ku, Fukuoka 814-0198, Japan

Received September 30, 2002; accepted December 17, 2002

Effects of a commercial polychlorinated biphenyls mixture, Kanechlor-500 (KC500), on the levels of serum thyroid hormones such as total thyroxine (T_4) and triiodothyronine (T_3) were examined comparatively in male Wistar rats and ddy mice. Serum T_4 levels were significantly decreased in both rats and mice 4 days after a single ip injection of KC500 (100 mg/kg body weight), whereas decreased levels of T_3 were observed in mice but not in rats. In addition, no significant change in the level of serum thyroid stimulating hormone was observed in either rats or mice. Hepatic UDP-glucuronosyltransferases (UDP-GTs) UGT1A1 and UGT1A6, which efficiently mediate glucuronidation of T_4 and promote the excretion of the hormones, were induced by KC500 in rats but not in mice. Hepatic microsomal cytochrome P450 (P450) content and the microsomal activity for 7-ethoxy-, 7-pentoxy-, and 7-benzoyloxy-resorufin dealkylations were significantly increased by KC500 in both rats and mice, although the magnitude of increase in the enzyme activities was higher in rats than in mice. The difference in the increase in the activity of microsomal enzymes, including UDP-GT and P450, between KC500-treated rats and mice was not correlated with that in the level of hepatic methylsulfonyl-PCB metabolites. In the present study, we found for the first time that the decrease in serum T_4 levels by KC-500 in mice occurred without increase in hepatic UDP-GTs, UGT1A1 and UGT1A6, responsible for T_4 glucuronidation. The present findings further suggested that although the decrease in serum T_4 levels in KC500-treated rats would occur at least in part through the induction of the UDP-GTs, it might not be dependent on only the increase in the enzymes.

Key Words: polychlorinated biphenyls; Kanechlor-500; thyroid hormones; UDP-glucuronosyltransferases; Wistar rats; ddy mice.

In 1968, an outbreak of accidental food poisoning caused by ingestion of Kanemi rice oil contaminated with commercial polychlorinated biphenyls (PCBs) occurred in western Japan, and the human toxicity of PCBs was confirmed. Some victims, called Yusho patients, continued to show various symptoms such as acneform eruptions, the hypersecretion of Meibomian glands, the hyperpigmentation of face, eyelids, and gingiva, and others (Kuratsune *et al.*, 1972), and 30 years later, Yusho patients still manifested the toxicity.

The worldwide commercial production of PCBs was banned in 1979, and yet, more than 70% of the global production of PCBs is estimated to be still in use or in stock (Hileman, 1993). Humans are continuously exposed to PCBs because of their presence in their accidental release from disposal sites (Phaneuf *et al.*, 1995) and in our diet, due in part to the accumulation of PCBs in certain species of fish and seafood collected in contaminated areas (Li and Hansen, 1997). Despite their gradual decline, PCBs exist as major contaminants of human tissues (Newsome *et al.*, 1995).

Toxicities of PCBs (Safe, 1990; Brouwer *et al.*, 1999), such as body weight loss, endocrine disruption, impairments of reproductive and immune systems, teratogenicity, and carcinogenicity, have been intensively studied over the last 30 years. Spectra of the toxicities are different between the species of animals (McConnell, 1989; Safe, 1994), and the species difference is believed to occur through the difference in their metabolism of PCBs (Duignan *et al.*, 1987, 1988). Decreases in serum thyroid hormones in rats by PCBs such as 3,3′,4,4′,5-pentachlorobiphenyl (3,3′,4,4′,5-pentaCB), Aroclor 1254, and 2,3,7,8-tetrachlorodibenzo-*p*-dioxin (TCDD) (Barter and Klaassen, 1994; Schuur *et al.*, 1997; Van Birgelen *et al.*, 1995) have been reported, and the decrease is thought to occur through PCB-mediated induction of hepatic UDP-glucuronosyltransferases (UDP-GTs), especially UGT1A1 and UGT1A6 (Visser, 1996). Likewise, some PCB congeners such as 2,3′,4,4′,5- and 3,3′,4,4′,5-pentaCBs and 2,2′,4,4′,5,5′- and 2,3,3′,4,4′,5-hexachlorobiphenyls (2,2′,4,4′,5,5′- and 2,3,3′,4,4′,5-hexaCBs) are reported to decrease the level of serum thyroid hormones and to increase the activity of hepatic drug-metabolizing enzymes in rats (Ness *et al.*, 1993; Van Birgelen *et al.*, 1995). We have also reported that nonplanar PCBs such as 2,2′,4,5,5′-pentaCB and 2,2′,3,3′,4,6′-hexaCB decrease the level of serum total thyroxine (T_4) in both rats and mice (Kato *et al.*, 2001). More

[1] To whom correspondence should be addressed. Fax: +81 54 264 56 35. E-mail: kato@ys7.u-shizuoka-ken.ac.jp.